SUPPORTING INFORMATION

Copper(II)-benzotriazole coordination compounds in click chemistry: A diagnostic reactivity study

Edward Loukopoulos,[a] Alaa Abdul-Sada,[a] Gizella Csire,[b] Csilla Kállay,[c] Adam Brookfield,[d] Graham J. Tizzard,[e] Simon J. Coles,[e] Ioannis N. Lykakis[f] and George E. Kostakis*[a]

[a] Department of Chemistry, School of Life Sciences, University of Sussex, Brighton BN1 9QJ, UK. E-mail: G.Kostakis@sussex.ac.uk

[b] Department of Inorganic and Analytical Chemistry, University of Debrecen, H-4032 Debrecen, Hungary.

[c] MTA-DE Redox and Homogeneous Catalytic Reaction

[d] School of Chemistry, The University of Manchester, Manchester M13 9PL, UK. Mechanisms Research Group, University of Debrecen, H-4032 Debrecen, Hungary.

[e] UK National Crystallography Service, Chemistry, University of Southampton SO1 71BJ, U.K

[f] Department of Chemistry, Aristotle University of Thessaloniki, Thessaloniki 54124, Greece

Table of contents	Page

Crystallographic Data

Table S1. Crystal data and structure refinement for ligands L^1, L^6, L^7.

Ligand	**L^1**	**L^6**	**L^7**
Empirical formula	$C_{20}H_{16}N_6$	$C_{14}H_{18}N_4O_2$	$C_{13}H_{11}N_3$
Formula weight	340.39	274.32	209.25
Temperature/K	100(2)	173.0	173.0
Crystal system	triclinic	triclinic	monoclinic
Space group	P-1	P-1	$P2_1/c$
a/Å	6.3881(4)	8.1128(8)	11.5768(16)
b/Å	7.6794(9)	8.7716(11)	5.9774(8)
c/Å	17.8944(12)	10.9028(11)	16.119(2)
α/°	87.348(7)	80.648(10)	90
β/°	89.529(5)	69.951(9)	106.541(14)
γ/°	67.155(8)	84.374(10)	90
Volume/Å^3	808.07(13)	718.41(15)	1069.3(3)
Z	2	2	4
ρ_{calc}g/cm^3	1.399	1.268	1.300
μ/mm^1	0.089	0.716	0.634
F(000)	356.0	292.0	440.0
Crystal size/mm^3	0.12 × 0.06 × 0.04	0.24 × 0.16 × 0.12	0.34 × 0.28 × 0.2
Radiation	Mo Kα (λ = 0.71075)	CuKα (λ = 1.54184)	CuKα (λ = 1.54184)
2Θ range for data collection/°	4.558 to 54.96	8.716 to 141.898	7.966 to 142.23
Index ranges	$-8 \le h \le 8$, $-9 \le k \le 9$, $-23 \le l \le 23$	$-9 \le h \le 7$, $-9 \le k \le 10$, $-13 \le l \le 12$	$-14 \le h \le 12$, $-5 \le k \le 7$, $-19 \le l \le 19$
Reflections collected	13024	3676	3132
Independent reflections	3650 [R_{int} = 0.0484, R_{sigma} = 0.0480]	2629 [R_{int} = 0.0358, R_{sigma} = 0.0721]	1981 [R_{int} = 0.0368, R_{sigma} = 0.0464]
Data/restraints/parameters	3650/0/235	2629/0/187	1981/0/145
Goodness-of-fit on F^2	1.118	0.986	1.034
Final R indexes [I>=2σ (I)]	R_1 = 0.0994, wR_2 = 0.2643	R_1 = 0.0484, wR_2 = 0.1108	R_1 = 0.0606, wR_2 = 0.1614
Final R indexes [all data]	R_1 = 0.1229, wR_2 = 0.2788	R_1 = 0.0730, wR_2 = 0.1284	R_1 = 0.0753, wR_2 = 0.1860
Largest diff. peak/hole / e Å^{-3}	0.68/-0.44	0.20/-0.26	0.20/-0.27

Table S2. Crystal data and structure refinement for compounds **1**-**5**.

Compound	**1**	**2**	**3**	**4**	**5**
Empirical formula	$C_{26}H_{22}CuF_6N_8O_6S_2$	$C_{46}H_{36}CuF_6N_8O_6S_2$	$C_{32}H_{31}CuF_6N_9O_6S_2$	$C_{36}H_{42.67}CuF_6N_8O_{9.33}S_2$	$C_{96}H_{88}Cu_4F_{12}N_{24}O_{16}S_4$
Formula weight	784.17	1038.49	879.32	978.43	2444.30
Temperature/K	173.0	173.0	100.0	100(2)	100(2)
Crystal system	triclinic	triclinic	monoclinic	monoclinic	triclinic
Space group	P-1	P-1	C2/c	$P2_1/n$	P-1
a/Å	9.3801(5)	9.0686(6)	14.1878(5)	20.8910(7)	16.6451(3)
b/Å	13.3284(8)	11.2199(6)	13.3086(5)	9.2748(2)	17.1433(2)
c/Å	16.0985(8)	12.0883(8)	40.4807(13)	25.1344(9)	19.1060(3)
α/°	107.132(5)	115.102(6)	90	90	90.7040(10)
β/°	103.696(5)	104.812(6)	90.608(3)	114.487(4)	90.0420(10)
γ/°	100.131(5)	93.484(5)	90	90	97.2670(10)
Volume/Å^3	1802.08(18)	1056.48(13)	7643.1(5)	4432.0(3)	5407.72(14)
Z	2	1	8	4	2
ρ_{calc}g/cm^3	1.445	1.632	1.528	1.466	1.501
μ/mm^1	2.659	2.439	0.765	2.336	2.420
F(000)	794.0	531.0	3592.0	2017.0	2496.0
Crystal size/mm^3	0.14 × 0.11 × 0.07	0.22 × 0.17 × 0.14	0.1 × 0.06 × 0.05	0.1 × 0.08 × 0.03	0.12 × 0.1 × 0.01
Radiation	CuKα (λ = 1.54184)	CuKα (λ = 1.54184)	MoKα (λ = 0.71073)	CuKα (λ = 1.54184)	CuKα (λ = 1.54178)
2Θ range for data collection/°	10.024 to 142.2	8.5 to 142.266	4.024 to 52.744	7.172 to 136.48	6.916 to 133.18
Index ranges	-11 ≤ h ≤ 11, -16 ≤ k ≤ 13, -13 ≤ l ≤ 19	-6 ≤ h ≤ 11, -13 ≤ k ≤ 13, -14 ≤ l ≤ 14	-17 ≤ h ≤ 17, -16 ≤ k ≤ 16, -50 ≤ l ≤ 50	-24 ≤ h ≤ 25, -11 ≤ k ≤ 10, -30 ≤ l ≤ 30	-19 ≤ h ≤ 19, -20 ≤ k ≤ 20, -22 ≤ l ≤ 22
Reflections collected	9434	5327	42305	41244	50455
Independent reflections	6550 [R_{int} = 0.0463, R_{sigma} = 0.0730]	3844 [R_{int} = 0.0921, R_{sigma} = 0.0976]	7794 [R_{int} = 0.0735, R_{sigma} = 0.0429]	8098 [R_{int} = 0.0843, R_{sigma} = 0.0564]	18266 [R_{int} = 0.0517, R_{sigma} = 0.0552]
Data/restraints/parameters	6550/0/444	3844/1/313	7794/0/506	8098/0/616	18266/1296/1442
Goodness-of-fit on F^2	1.048	1.048	1.029	1.007	1.010
Final R indexes [I>=2σ (I)]	R_1 = 0.0657, wR_2 = 0.1742	R_1 = 0.0682, wR_2 = 0.1736	R_1 = 0.0938, wR_2 = 0.2448	R_1 = 0.0606, wR_2 = 0.1638	R_1 = 0.0609, wR_2 = 0.1626
Final R indexes [all data]	R_1 = 0.0890, wR_2 = 0.1921	R_1 = 0.0883, wR_2 = 0.1948	R_1 = 0.1173, wR_2 = 0.2638	R_1 = 0.0765, wR_2 = 0.1744	R_1 = 0.0818, wR_2 = 0.1769
Largest diff. peak/hole / e Å^{-3}	1.66/-0.65	1.06/-0.81	1.59/-0.89	1.48/-1.02	1.06/-0.55

Table S3. Crystal data and structure refinement for triazoles **18aa** – **18ad**.

Triazole	**18aa**	**18ab**	**18ac**	**18ad**
Empirical formula	$C_{15}H_{13}N_3$	$C_{16}H_{15}N_3O$	$C_{13}H_{17}N_3$	$C_{10}H_{11}N_3O$

Formula weight	235.28	265.31	215.29	189.22
Temperature/K	173.0	173.0	173.0	173.0
Crystal system	orthorhombic	monoclinic	monoclinic	triclinic
Space group	$Pna2_1$	$P2_1$	$P2_1/c$	P-1
a/Å	11.2241(4)	8.1339(8)	13.0813(10)	8.2035(12)
b/Å	19.3350(6)	5.6565(6)	5.4875(3)	11.0403(11)
c/Å	5.5817(2)	14.5299(16)	17.7677(16)	11.2020(11)
α/°	90	90	90	93.064(8)
β/°	90	92.836(9)	108.906(9)	106.687(11)
γ/°	90	90	90	104.934(10)
Volume/Å^3	1211.33(7)	667.69(12)	1206.62(17)	930.1(2)
Z	4	2	4	4
ρ_{calc}g/cm^3	1.290	1.320	1.185	1.351
μ/mm^1	0.619	0.680	0.563	0.744
F(000)	496.0	280.0	464.0	400.0
Crystal size/mm^3	0.24 × 0.18 × 0.1	0.27 × 0.1 × 0.06	0.28 × 0.19 × 0.16	0.12 × 0.08 × 0.06
Radiation	CuKα (λ = 1.54184)	CuKα (λ = 1.54184)	CuKα (λ = 1.54184)	CuKα (λ = 1.54184)
2Θ range for data collection/°	9.11 to 142.246	10.89 to 140.486	10.636 to 140.672	8.32 to 142.388
Index ranges	-12 ≤ h ≤ 13, -15 ≤ k ≤ 23, -6 ≤ l ≤ 6	-9 ≤ h ≤ 9, -5 ≤ k ≤ 6, -17 ≤ l ≤ 14	-15 ≤ h ≤ 15, -4 ≤ k ≤ 6, -21 ≤ l ≤ 20	-10 ≤ h ≤ 8, -11 ≤ k ≤ 13, -13 ≤ l ≤ 11
Reflections collected	3555	1972	3667	5011
Independent reflections	2053 [R_{int} = 0.0254, R_{sigma} = 0.0382]	1586 [R_{int} = 0.0309, R_{sigma} = 0.0578]	2234 [R_{int} = 0.0350, R_{sigma} = 0.0433]	3462 [R_{int} = 0.0266, R_{sigma} = 0.0545]
Data/restraints/parameters	2053/1/163	1586/1/183	2234/0/146	3462/0/255
Goodness-of-fit on F^2	1.069	1.019	1.024	1.052
Final R indexes [I>=2σ (I)]	R_1 = 0.0373, wR_2 = 0.0855	R_1 = 0.0464, wR_2 = 0.1051	R_1 = 0.0469, wR_2 = 0.1150	R_1 = 0.0451, wR_2 = 0.1051
Final R indexes [all data]	R_1 = 0.0418, wR_2 = 0.0892	R_1 = 0.0617, wR_2 = 0.1164	R_1 = 0.0658, wR_2 = 0.1336	R_1 = 0.0688, wR_2 = 0.1216
Largest diff. peak/hole / e Å^{-3}	0.10/-0.17	0.19/-0.19	0.14/-0.19	0.18/-0.24

Additional figures of crystal structures

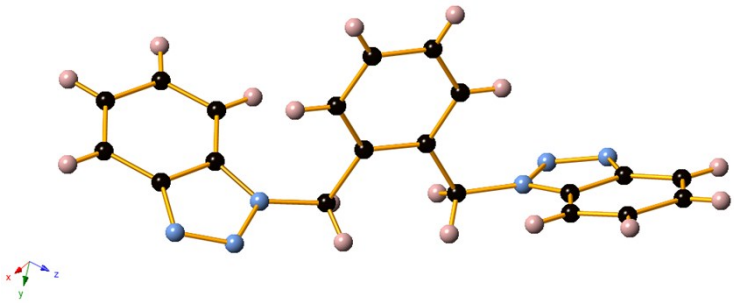

Figure S1. The structure of L^1. Colour code C (black), H (light pink), N (light blue).

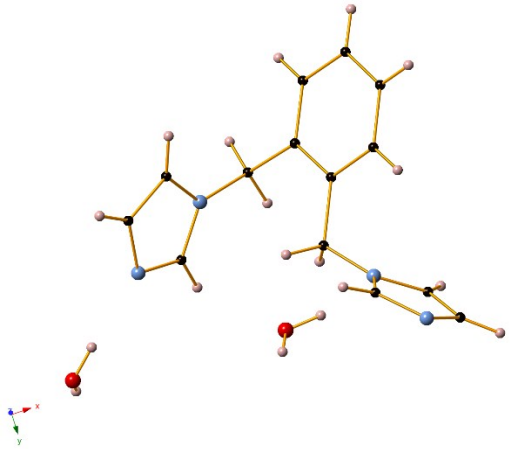

Figure S2. The structure of $L^6 \cdot 2H_2O$. Colour code C (black), H (light pink), N (light blue), O (red).

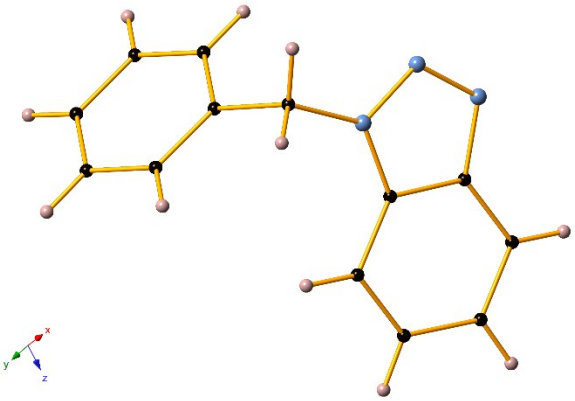

Figure S3. The structure of L^7. Colour code C (black), H (light pink), N (light blue).

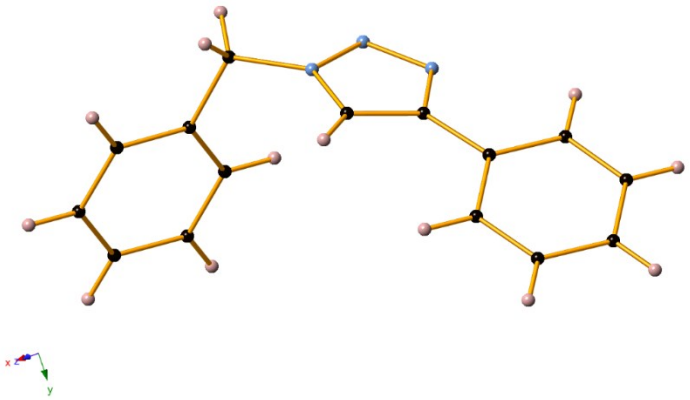

Figure S4. The structure of triazole **18aa**. Colour code C (black), H (light pink), N (light blue).

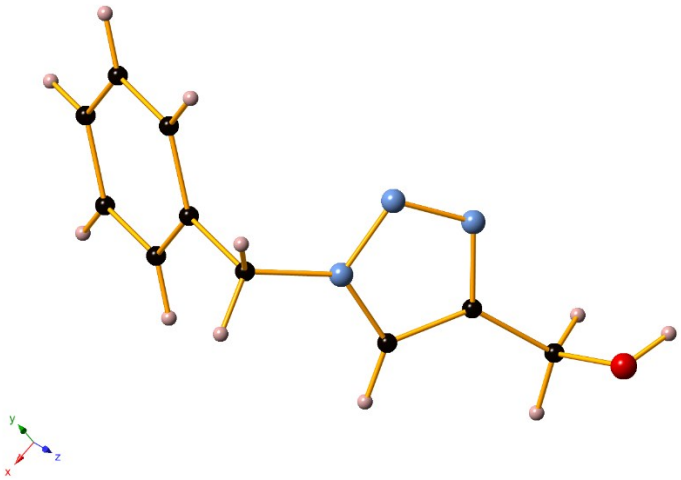

Figure S5. The structure of triazole **18ab**. Colour code C (black), H (light pink), N (light blue), O (red).

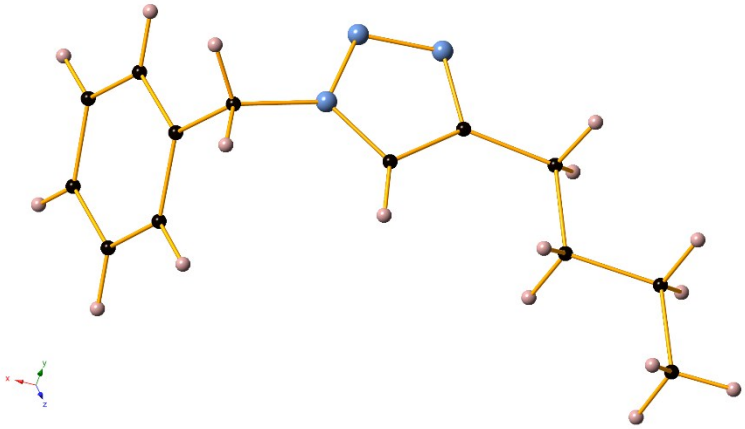

Figure S6. The structure of triazole **18ac**. Colour code C (black), H (light pink), N (light blue).

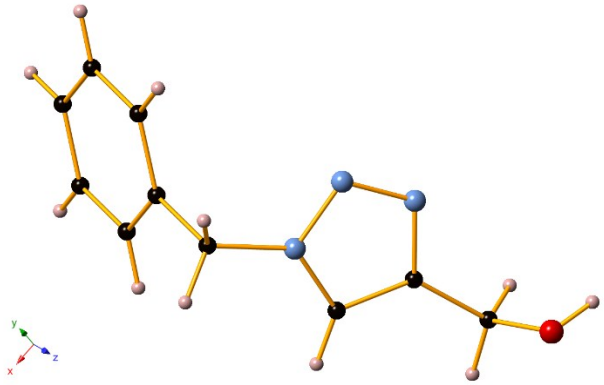

Figure S7 The structure of triazole **18ad**. Colour code C (black), H (light pink), N (light blue), O (red).

Characterization data for ligands L^5 - L^7

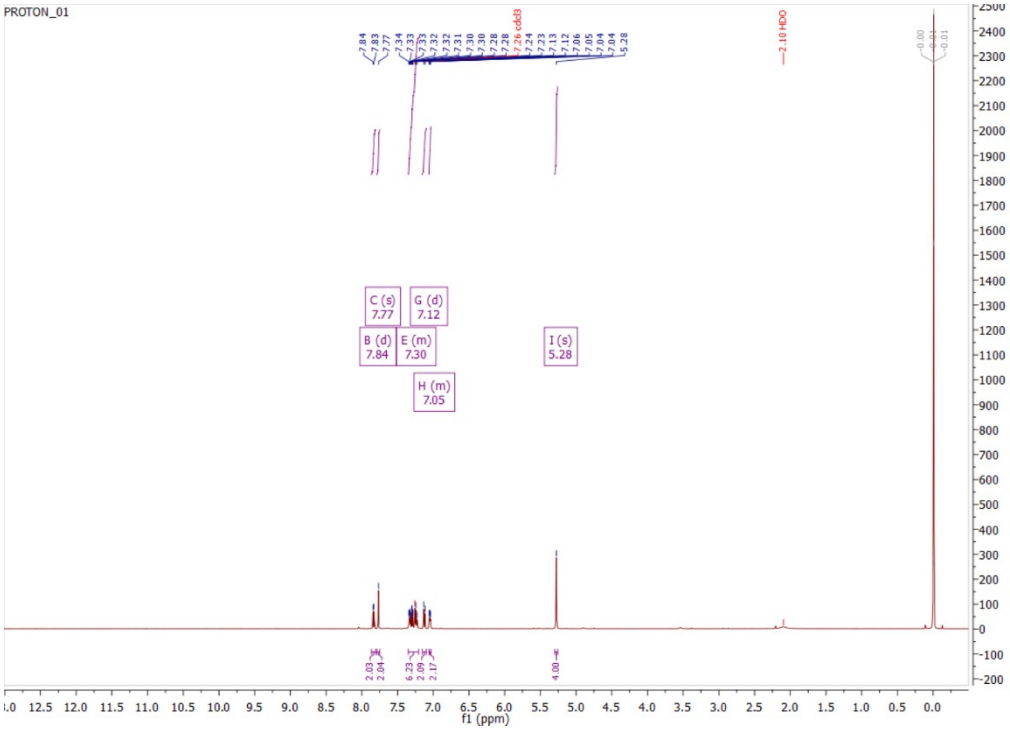

Figure S8. ^{1}H NMR spectrum of L^5.

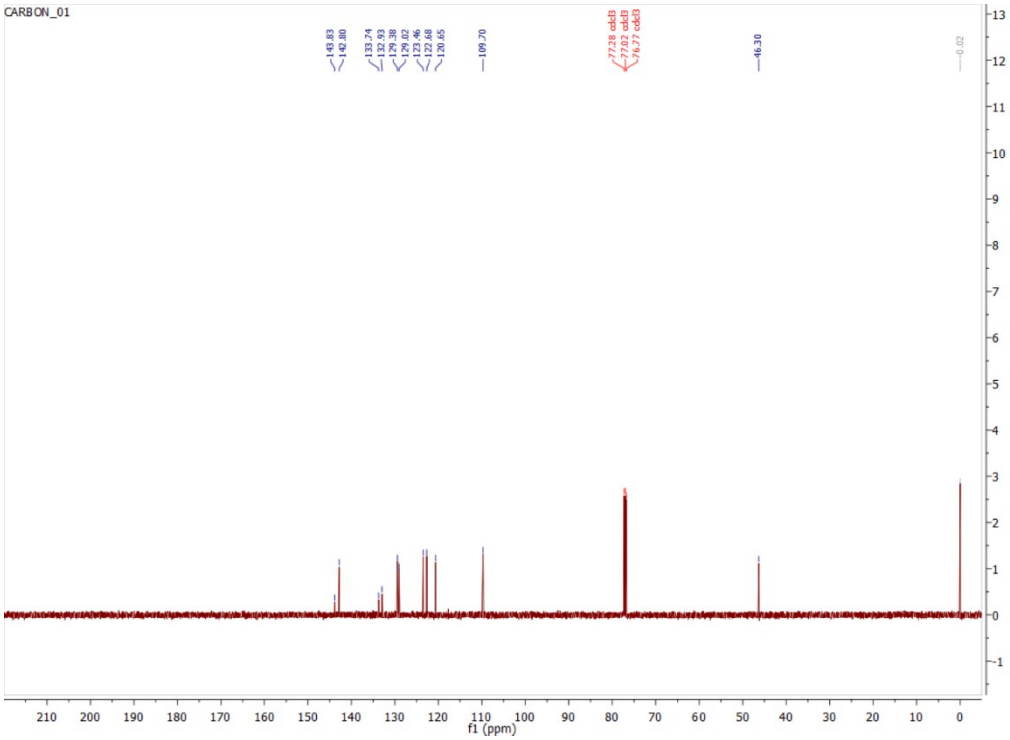

Figure S9. ^{13}C NMR spectrum of L^5.

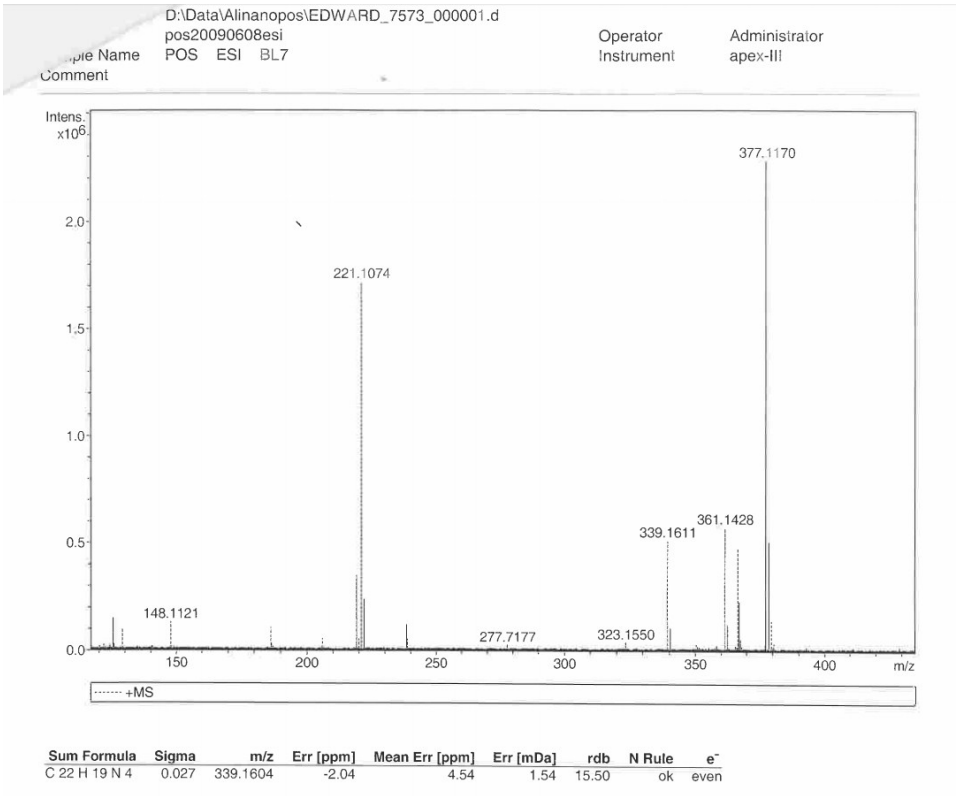

Figure S10. HRMS spectrum of L^5.

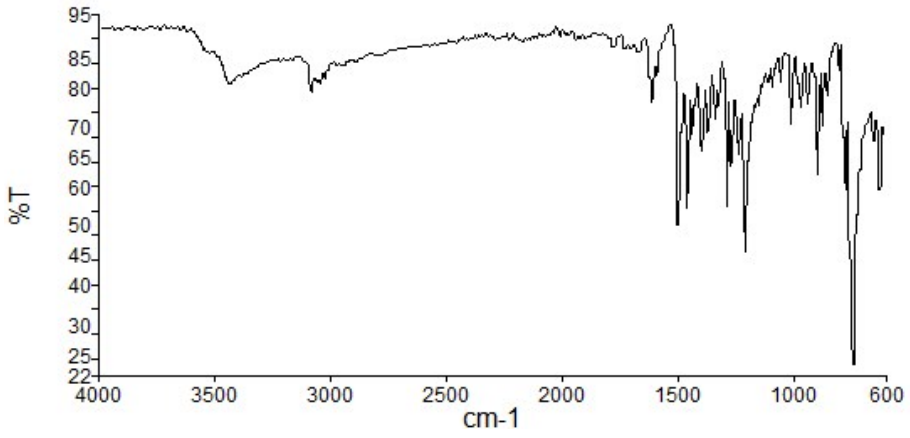

Figure S11. IR spectrum of L^5.

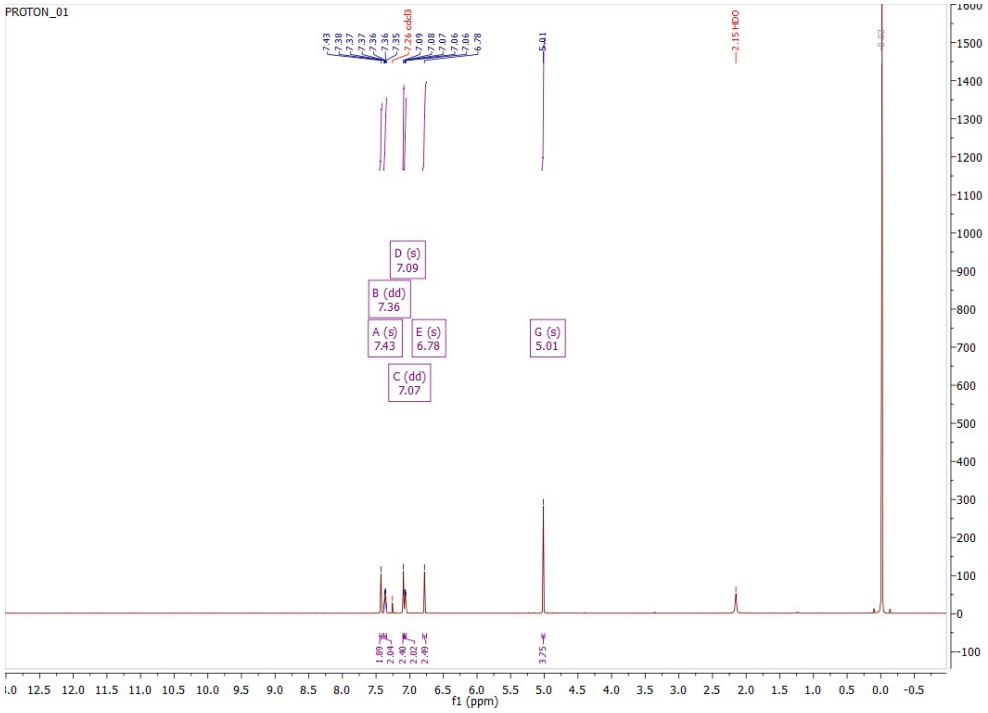

Figure S12. ^{1}H NMR spectrum of L^{6}.

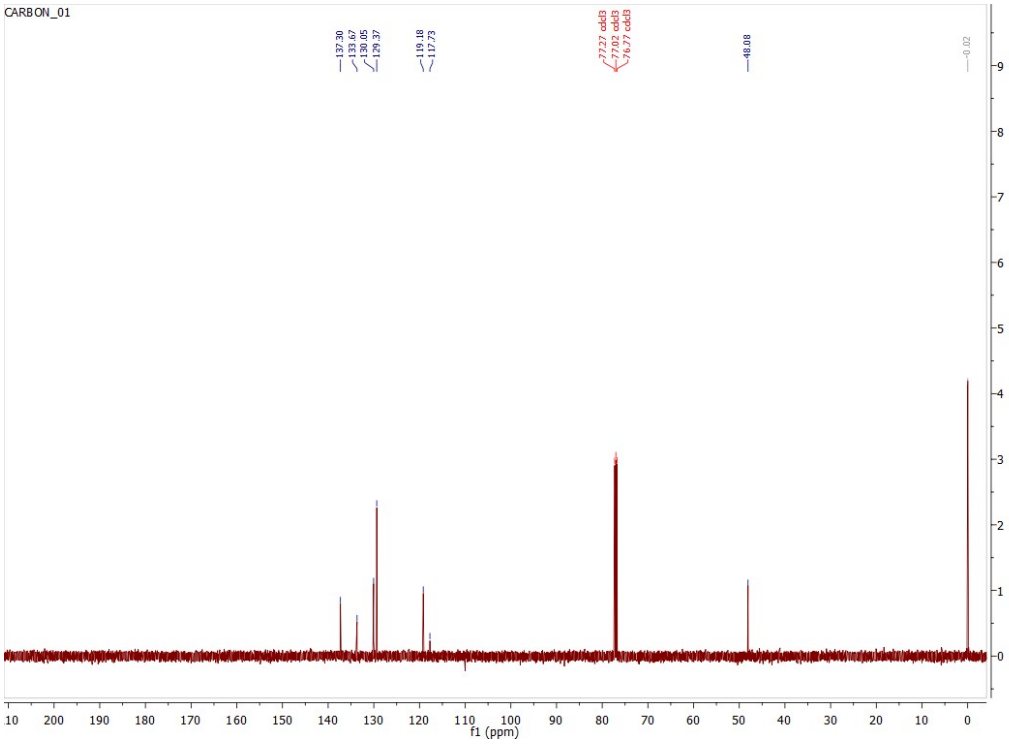

Figure S13. ^{13}C NMR spectrum of L^{6}.

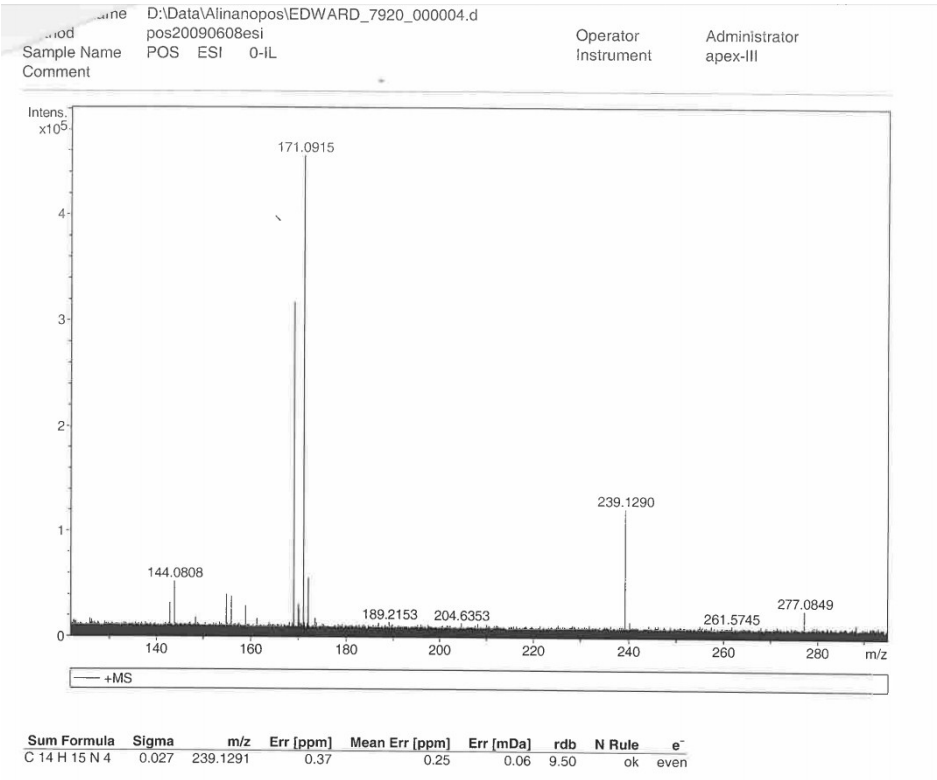

Figure S14. HRMS spectrum of L[6].

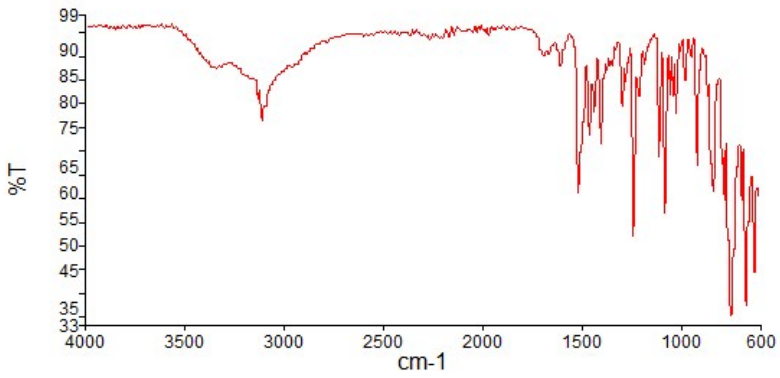

Figure S15. IR spectrum of L[6].

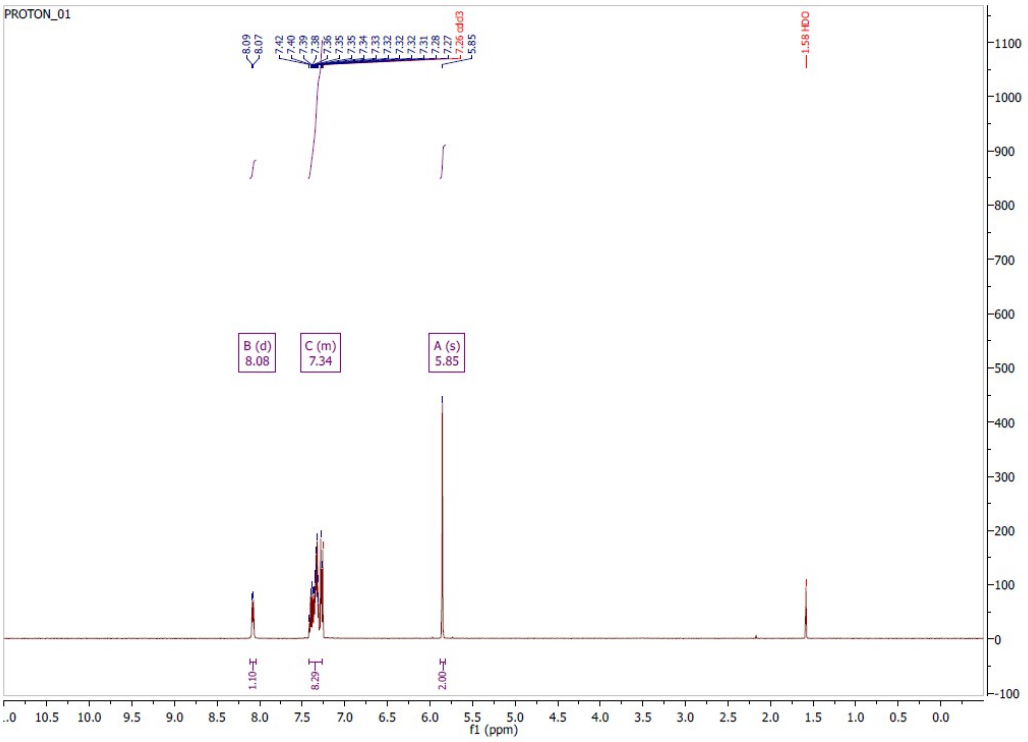

Figure S16. ^{1}H NMR spectrum of L^{7}.

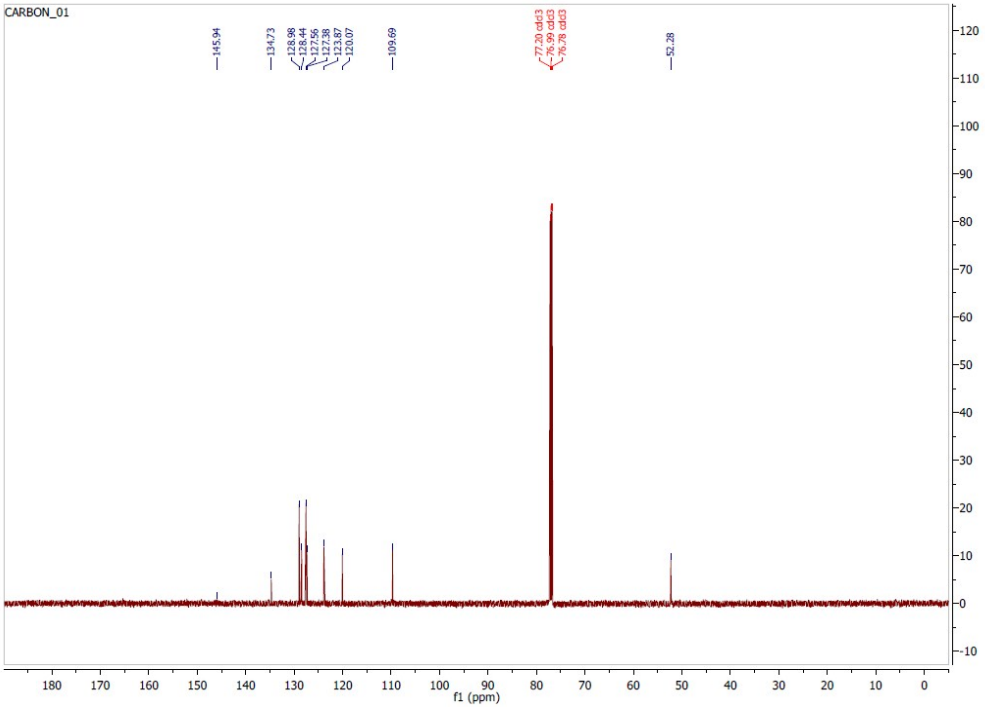

Figure S17. ^{13}C NMR spectrum of L^{7}.

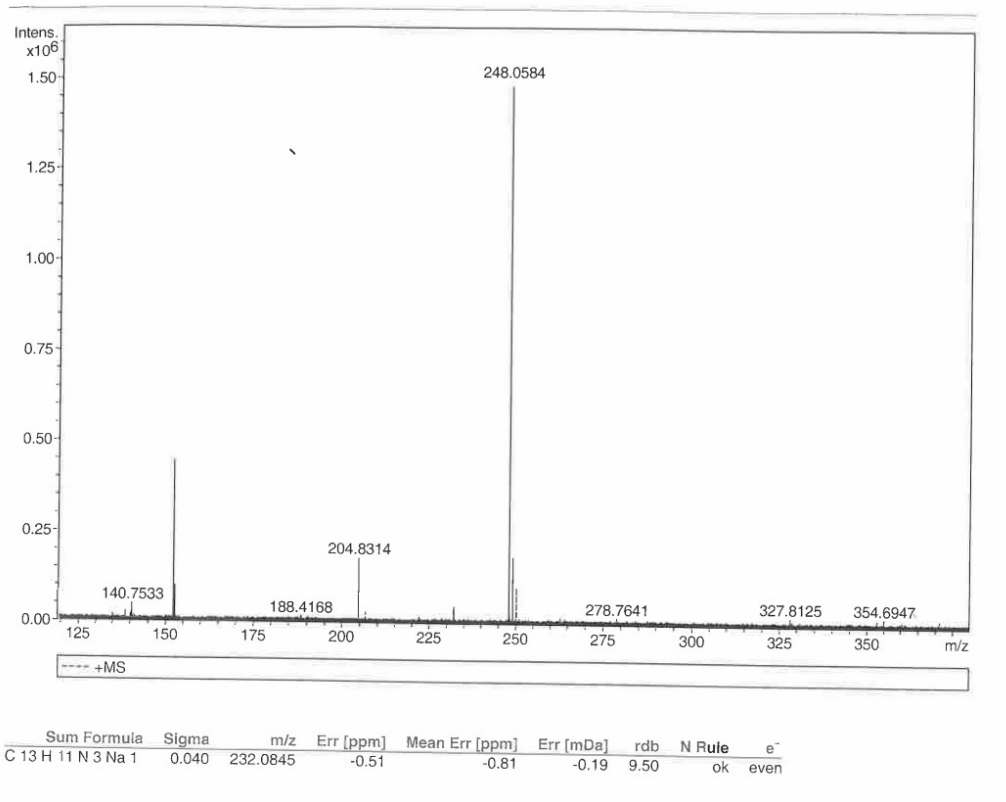

Figure S18. HRMS spectrum of L^7.

Characterization data of the Cu compounds

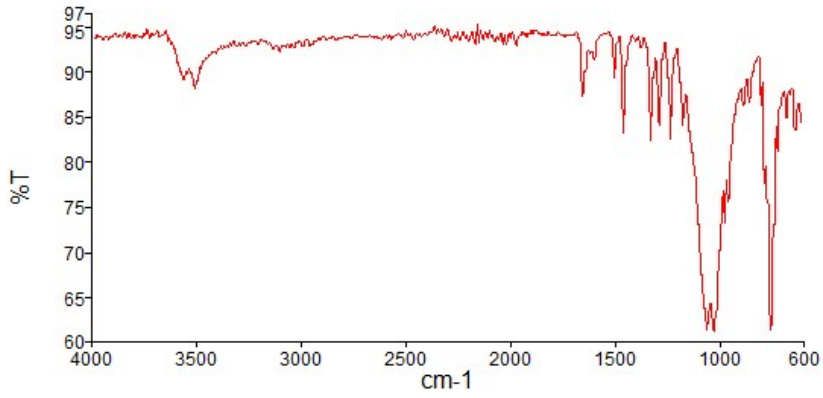

Figure S19. IR spectrum of **1**.

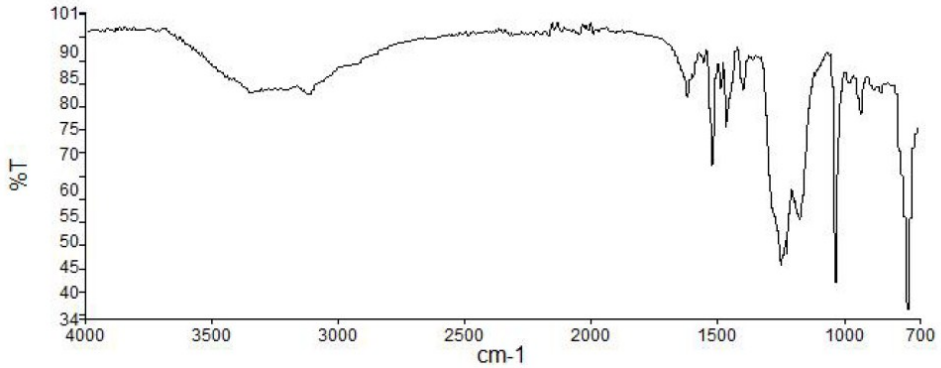

Figure S20. IR spectrum of **2**.

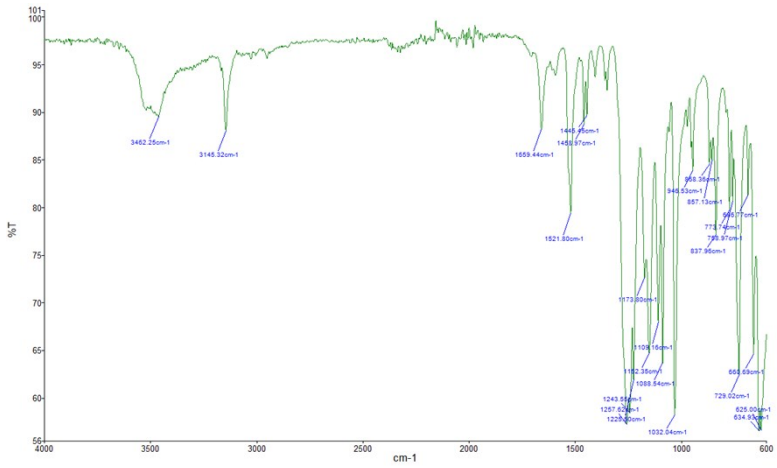

Figure S21. IR spectrum of **3**.

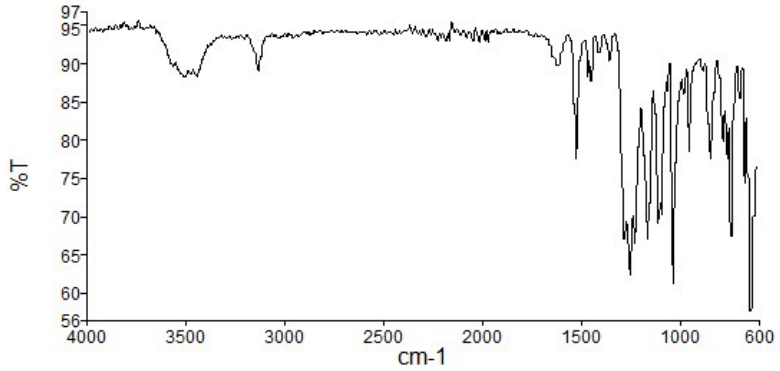

Figure S22. IR spectrum of **4**.

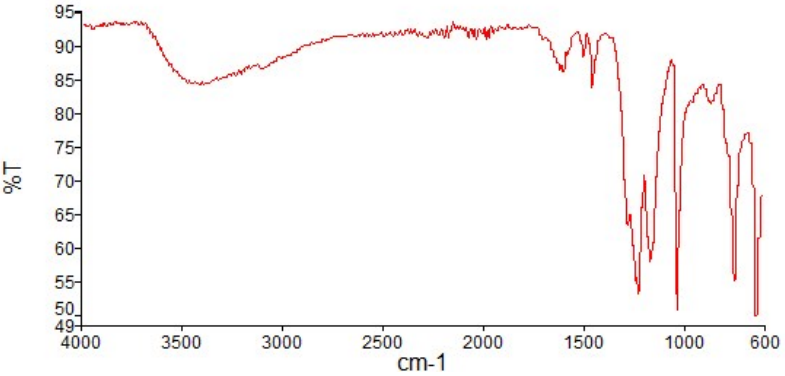

Figure S23. IR spectrum of **5**.

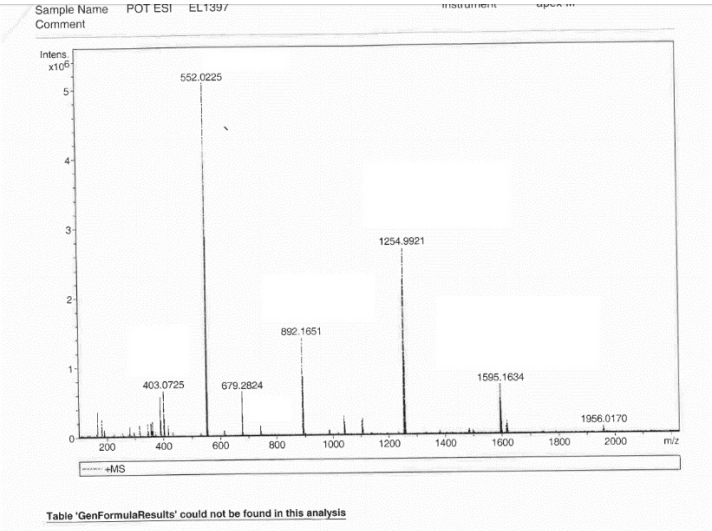

Figure S24. ESI-MS data for compound **1** in methanol. Main fragments: 403.07 m/z $[Cu(L^4)]^+$, 552.02 m/z $[Cu(L^4)(CF_3SO_3)]^+$, 614.96 m/z $[Cu_2(L^4)(CF_3SO_3)]^+$, 679.28 m/z $[Cu_3(L^4)(CF_3SO_3)]^+$, 743.22 m/z $[Cu(L^4)_2]^+$, 892.17 m/z $[Cu(L^4)_2(CF_3SO_3)]^+$, 1040.12 m/z $[Cu(L^4)_2(CF_3SO_3)_2]^+$, 1106.07 m/z $[Cu_2(L^4)_2(CF_3SO_3)_2]^+$, 1232.35 m/z $[Cu(L^4)_3(CF_3SO_3)]^+$, 1254.99 m/z $[Cu_2(L^4)_2(CF_3SO_3)_3]^+$, 1595.16 m/z $[Cu_2(L^4)_3(CF_3SO_3)_3]^+$, 1956.02 m/z $[Cu_4(L^4)_5]^+$.

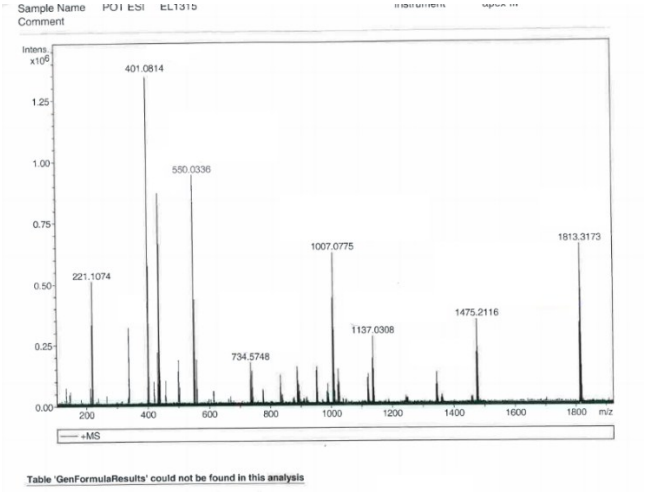

Figure S25. ESI-MS data for compound **2** in methanol. Main fragments: 339.16 m/z $[(L^5)+H]^+$, 401.08 m/z $[Cu(L^5)]^+$, 437.05 m/z $[Cu(L^5)(H_2O)_2]^+$, 464.03 m/z $[Cu_2(L^5)]^+$, 500.08 m/z $[Cu_2(L^5)(H_2O)_2]^+$, 550.03 m/z $[Cu(L^5)(CF_3SO_3)]^+$, 612.96 m/z $[Cu_2(L^1)(CF_3SO_3)]^+$, 734.57 m/z $[Cu(L^5)(CF_3SO_3)_2(H_2O)_2]^+$, 739.25 m/z $[Cu(L^5)_2]^+$, 888.19 m/z $[Cu(L^1)_2(CF_3SO_3)]^1$, 953.11 m/z $[Cu_2(L^1)_2(CF_3SO_3)]^+$, 1007.08 m/z $[Cu_2(L^1)_2(CF_3SO_3)(H_2O)_3]^+$, 1037.14 m/z $[Cu(L^1)_2(CF_3SO_3)_2]^+$, 1120.10 m/z $[Cu_2(L^5)_2(CF_3SO_3)_2(H_2O)]^+$, 1137.03 m/z $[Cu_2(L^5)_2(CF_3SO_3)_2(H_2O)_2]^+$, 1245.19 m/z $[Cu(L^5)_3(CF_3SO_3)_2(H_2O)]^+$, 1350.00 m/z $[Cu_3(L^5)_2(CF_3SO_3)_3(H_2O)_2]^+$, 1475.21 m/z $[Cu_2(L^5)_3(CF_3SO_3)_2(H_2O)_2]^+$, 1813.32 m/z $[Cu_2(L^5)_4(CF_3SO_3)_2(H_2O)_2]^+$.

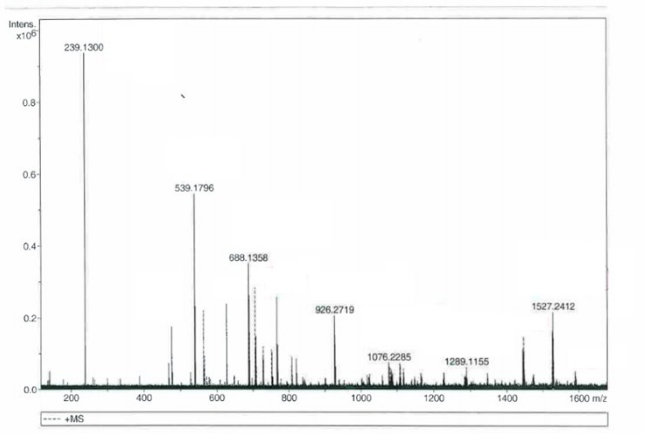

Figure S26. ESI-MS data for compound **3** in methanol. Main fragments: 239.13 m/z $[(L^6)+H]^+$, 301.05 m/z $[Cu(L^6)]^+$, 360.06 m/z $[Cu(L^6)_2(CF_3SO_3)(MeOH)]^{2+}$, 450.00 m/z $[Cu(L^6)(CF_3SO_3)]^+$, 477.26 m/z $[(L^6)_2+H]^+$, 539.18 m/z $[Cu(L^6)_2]^+$, 598.18 m/z $[Cu(L^6)(CF_3SO_3)_2]^+$, 627.22 m/z $[(L^6)_2(CF_3SO_3)]^+$, 688.14 m/z $[Cu(L^6)_2(CF_3SO_3)]^+$, 715.36 m/z $[(L^6)_3+H]^+$, 737.36 m/z $[(L^6)_3+Na]$, 753.07 m/z $[Cu_2(L^6)_2(CF_3SO_3)]^+$, 777.39 m/z $[Cu(L^6)_3]^+$, 808.20 m/z $[Cu(L^6)_3(MeOH)]^+$, 838.09 m/z

$[Cu(L^6)_2(CF_3SO_3)_2]^+$, 902.00 m/z $[Cu_2(L^6)_2(CF_3SO_3)_2]^+$, 926.27 m/z $[Cu(L^6)_3(CF_3SO_3)]^+$, 1018.22 m/z $[Cu(L^6)_2(CF_3SO_3)_3(MeOH)]^+$, 1076.23 m/z $[Cu(L^6)_3(CF_3SO_3)_2]^+$, 1164.40 m/z $[(L^6)_3(CF_3SO_3)_3]^+$, 1224.78 m/z $[Cu(L^6)_3(CF_3SO_3)_3]^+$, 1289.12 m/z $[Cu_2(L^6)_3(CF_3SO_3)_3]^+$, 1352.34 m/z $[Cu_3(L^6)_3(CF_3SO_3)_3]^+$, 1445.63 m/z $[Cu_3(L^6)_4(CF_3SO_3)_2]^+$, 1527.24 m/z $[Cu_2(L^6)_4(CF_3SO_3)_3]^+$, 1589.32 m/z $[Cu_3(L^6)_4(CF_3SO_3)_3]^+$.

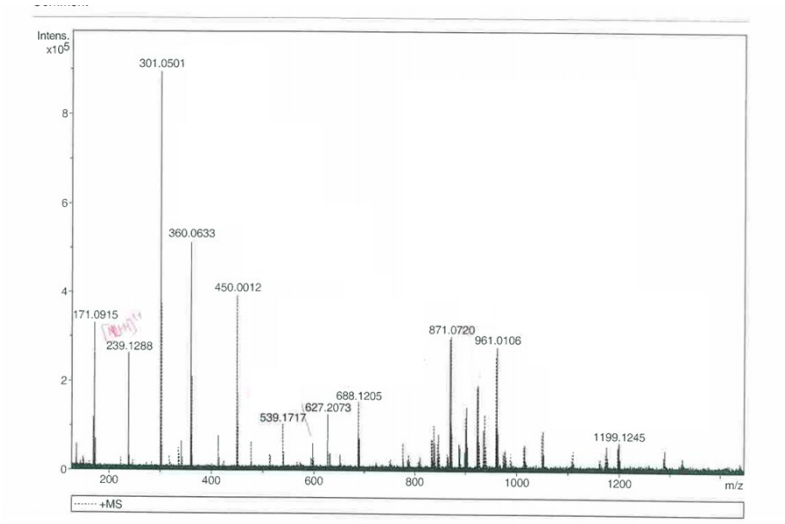

Figure S27. ESI-MS data for compound **4** in methanol. Main fragments: Main fragments: 239.13 m/z $[(L^6)+H]^+$, 301.05 m/z $[Cu(L^6)]^+$, 360.06 m/z $[Cu(L^6)_2(CF_3SO_3)(MeOH)]^{2+}$, 450.00 m/z $[Cu(L^6)(CF_3SO_3)]^+$, 539.17 m/z $[Cu(L^6)_2]^+$, 598.18 m/z $[Cu(L^6)(CF_3SO_3)_2]^+$, 627.21 m/z $[(L^6)_2(CF_3SO_3)]^+$, 688.12 m/z $[Cu(L^6)_2(CF_3SO_3)]^+$, 838.09 m/z $[Cu(L^6)_2(CF_3SO_3)_2]^+$, 871.07 m/z $[Cu(L^6)_2(CF_3SO_3)_2(MeOH)]^+$, 902.00 m/z $[Cu_2(L^6)_2(CF_3SO_3)_2]^+$, 925.04 m/z $[Cu(L^6)_3(CF_3SO_3)]^+$, 961.01 m/z $[Cu_3(L^6)(CF_3SO_3)_2]^+$, 986.04 m/z $[Cu(L^6)_2(CF_3SO_3)_3]^+$, 1050.95 m/z $[Cu_2(L^6)_2(CF_3SO_3)_3]^+$, 1199.12 m/z $[Cu_3(L^6)_3(CF_3SO_3)_2]^+$.

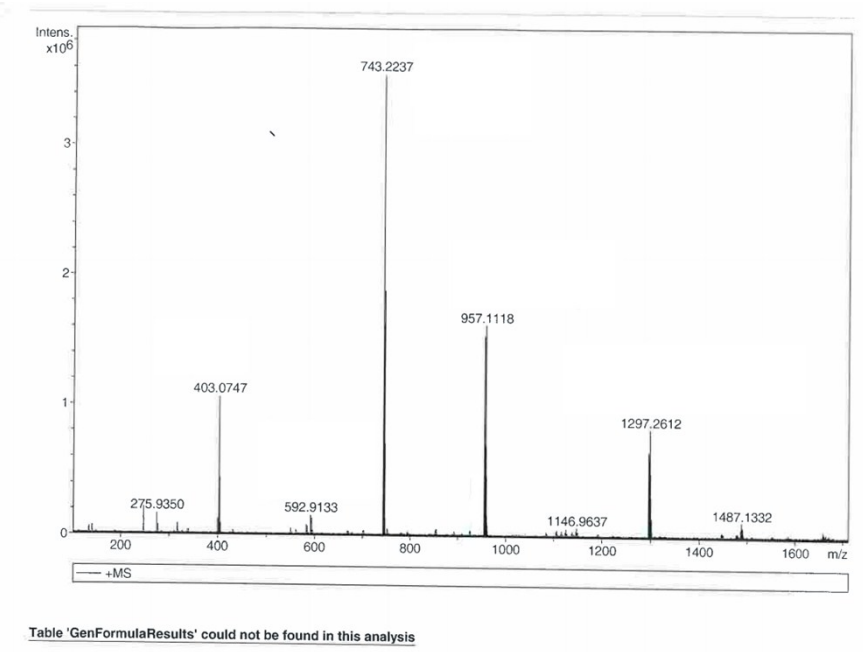

Figure S28. ESI-MS data for compound **5** in methanol. Main fragments: 403.07 m/z $[Cu(L^1)]^+$, 592.91 m/z $[Cu(L^1)_2(CF_3SO_3)_3]^{2+}$, 743.22 m/z $[Cu(L^1)_2]^+$, 957.11 m/z $[Cu_2(L^1)_2(CF_3SO_3)]^+$, 1297.26 m/z $[Cu_2(L^1)_3(CF_3SO_3)]^+$.

TGA Analysis. Compound **1** undergoes an initial mass loss (4.68%) in the 100-125°C range that is attributed to the loss of any remaining acetonitrile solvent with good agreement (theoretical value of 5.01%). The second mass loss (86.28%) occurs at approximately 285°C as the existing core begins to decompose to the resulting oxide (theor.: 84.31%). Compound **2** completely retains its stability up to the region of 260°C. At that point, a mass loss of 28.77% occurs gradually due to the removal of the triflate anions, with excellent agreement to the theoretical value (28.70%). The remaining polymeric core loses its stability at approximately 375°C and is subjected to gradual decomposition to CuO. Once again, the found (63.93%) and theoretical (63.64%) values for this mass loss are in very good agreement. In the case of compound **3**, there is an immediate mass loss (5.997%) which concludes at 163°C and is owed to the loss of the coordinated acetonitrile molecule with satisfactory agreement (theoretical: 4.02%). The left residue remains stable until approximately 300°C before it begins decomposition. The TGA analysis of compound **4** is in agreement with the elemental analysis measurements which suggest that the acetone molecules in the lattice are removed under room

temperature. As such, the first mass loss in the range of 85-100°C is attributed to the removal of the coordinated water solvent from the framework. The remaining core is stable until it begins decomposing in the region of 300-325°C to the eventual oxide residue. The total mass loss for these processes (92.84%) is in very good agreement to the theoretical value (90.71%). Finally, in compound **5** there is a continuous mass loss which occurs immediately, until approximately 217°C. This corresponds to the loss of the remaining four acetone solvent molecules that are present in the lattice (found: 9.54%, theoretical: 9.50%). An immediate second mass loss occurs after this, as the remaining framework is decomposed.

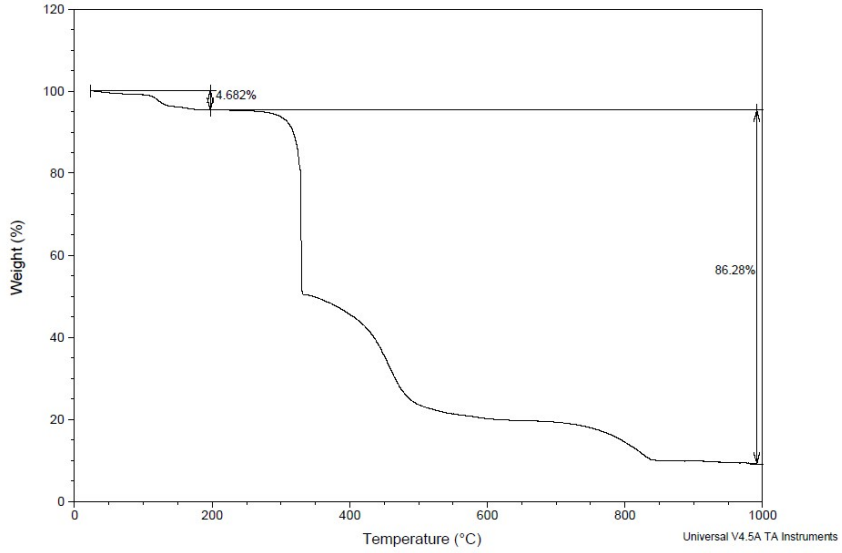

Figure S29. TGA graph for compound **1**.

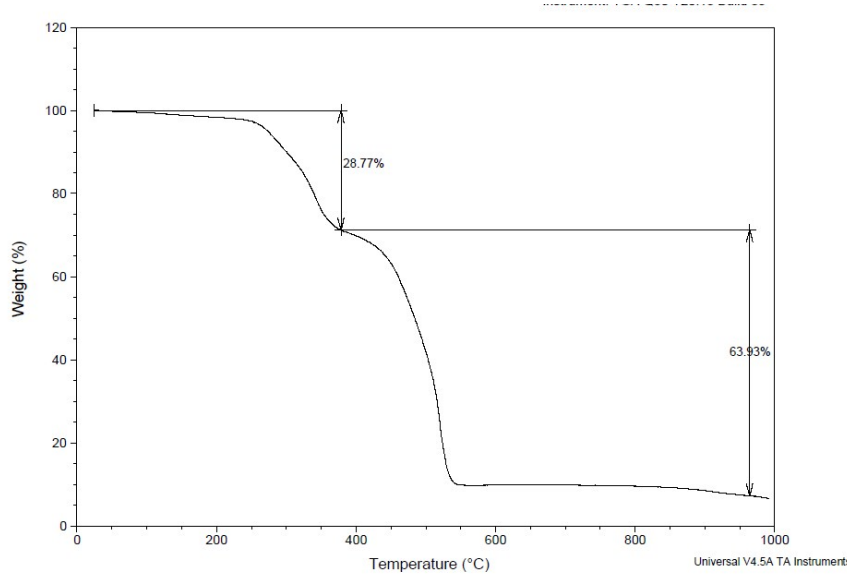

Figure S30. TGA graph for compound **2**.

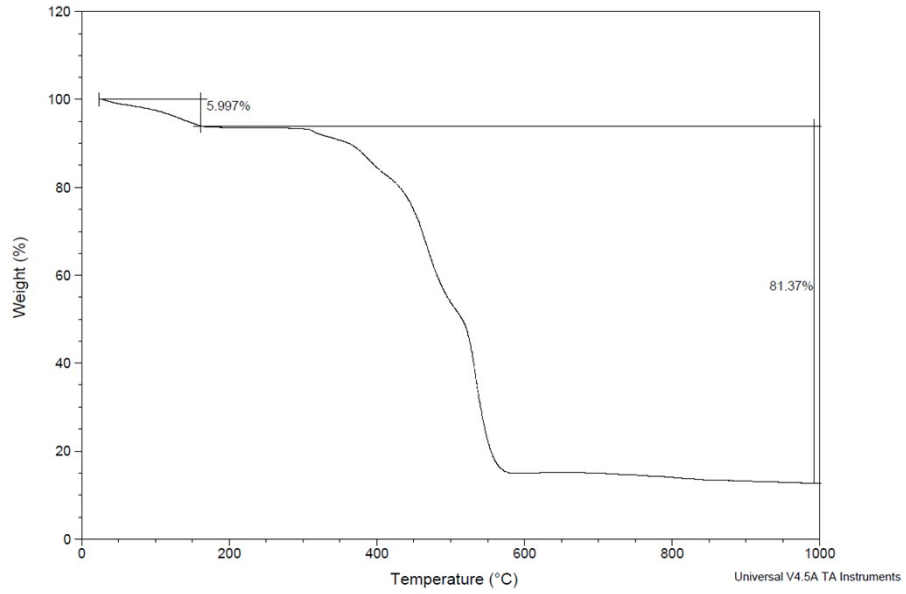

Figure S31. TGA graph for compound **3**.

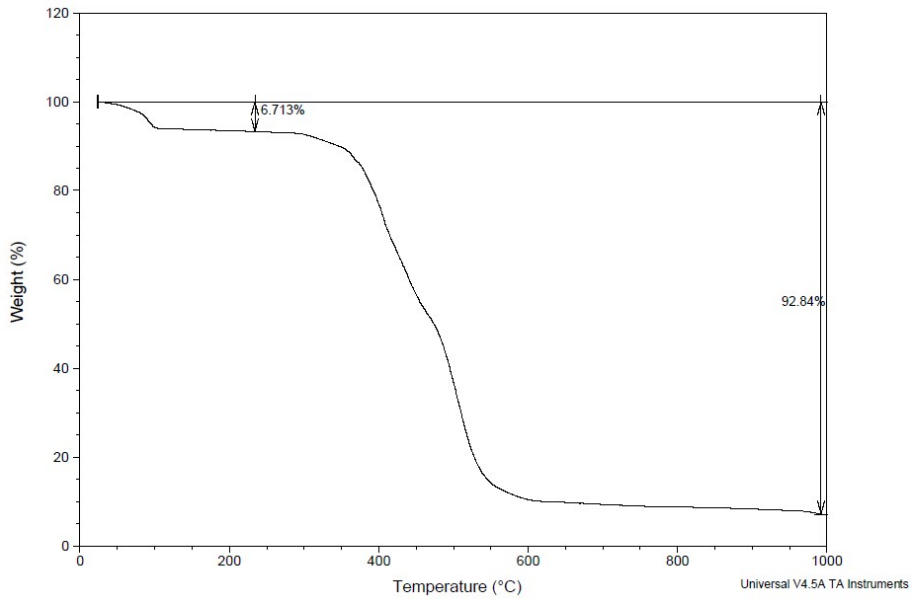

Figure S32. TGA graph for compound **4**.

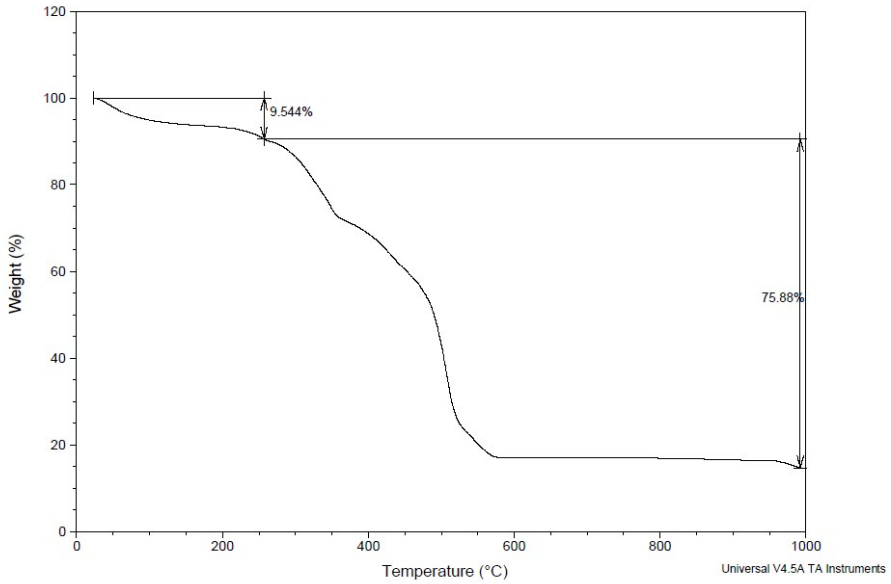

Figure S33. TGA graph for compound **5**.

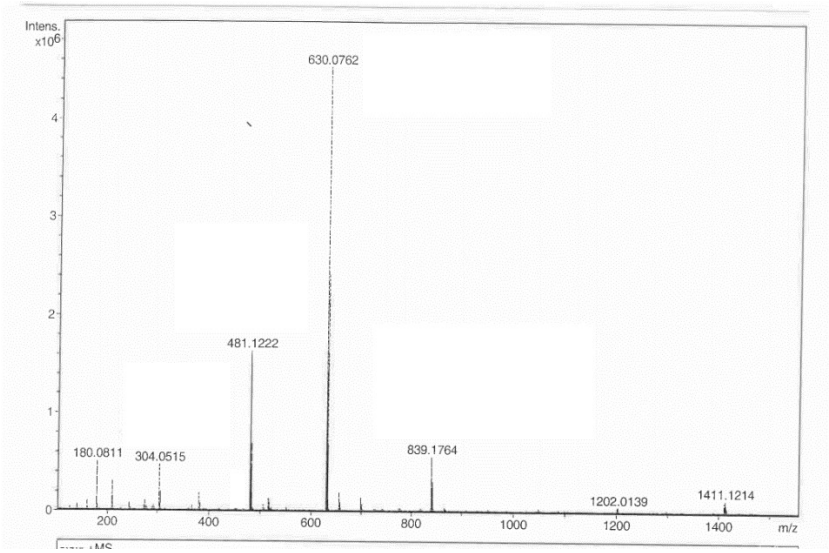

Figure S34. ESI-MS data for the *in situ* generated catalyst from $Cu(OTf)_2 \cdot H_2O$ and L^7 in methanol. Main fragments: 304.05 m/z $[Cu(L^7)(MeOH)]^{+1}$, 481.12 m/z $[Cu(L^7)_2]^{1+}$, 630.08 m/z $[Cu(L^7)_2(CF_3SO_3)]^{+1}$, 839.18 m/z $[Cu(L^7)_3(CF_3SO_3)]^{+1}$, 1048.27 m/z $[Cu(L^7)_4(CF_3SO_3)]^{+1}$, 1202.01 m/z $[Cu_2(L^7)_3(CF_3SO_3)_3]^{+1}$, 1411.12 m/z $[Cu_2(L^7)_4(CF_3SO_3)_3]^{+1}$.

Table S4. The electrochemical data of the Cu(II) complexes **2**, **10**, **12** (Parameters of the voltammetric measurements: glassy carbon electrode, DMF or DMSO, 0.1 M TBAP, 100 mV/s).

Complex	E_c (V)	I_c (μA)	E_a (V)	I_a (μA)	ΔE (V)	$E_{1/2}$ (V)	E^0 (V)	I_a/I_k	Solvent
Compound **12**	0.345	-7.1	0.464	19.6					DMF
	0.0507	-16.8	0.182	73.1					
	-0.215	-24.6							
Compound **10**	0.429	-6.91	0.556	8.45	0.127	0.493	0.702	1.2	
Compound **2**	0.409	-13.5	0.528	16.5	0.119	0.469	0.678	1.2	
$Cu(NO_3)_2$	0.371	-8.75	0.529	16.5					
	-0.0137	-14.9	0.182	32.6					
	-0.243	-15.1							
Compound **12**	0.224	-4.73	0.436	9.92					DMSO
	0.0185	-12.8	0.133	27.4					
	-0.392	-15.1	0.07	35.9					
Compound **10**	0.22	-3.07	0.45	3.31	0.23	0.335	0.544	1.1	
Compound **2**	0.22	-11.8	0.443	12.1	0.223	0.332	0.541	1.0	
$Cu(NO_3)_2$	0.226	-4.48	0.44	9.55					
	0.0251	-15.5	0.158	32.1					
	-0.321	-24	0.081	47.2					

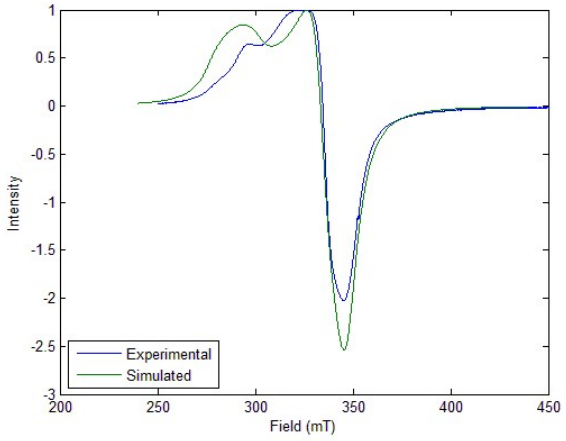

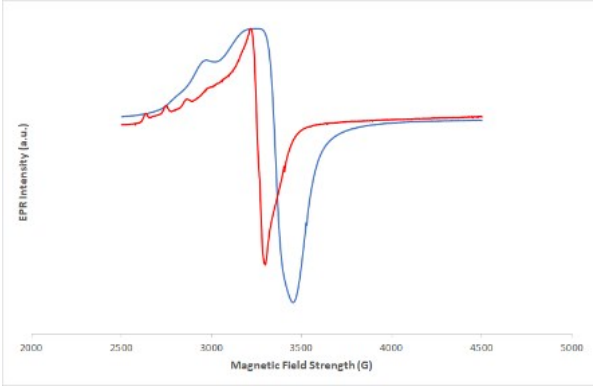

Figure S35. (left) Experimental (blue traces) and simulated (green traces) X-band EPR spectra for **2** at 9.496899 GHz and 5 K. (right) Overlay of EPR spectra in solid state (blue traces) and in methanolic solution (red traces) for **2** at 9.496899 GHz and 5 K.

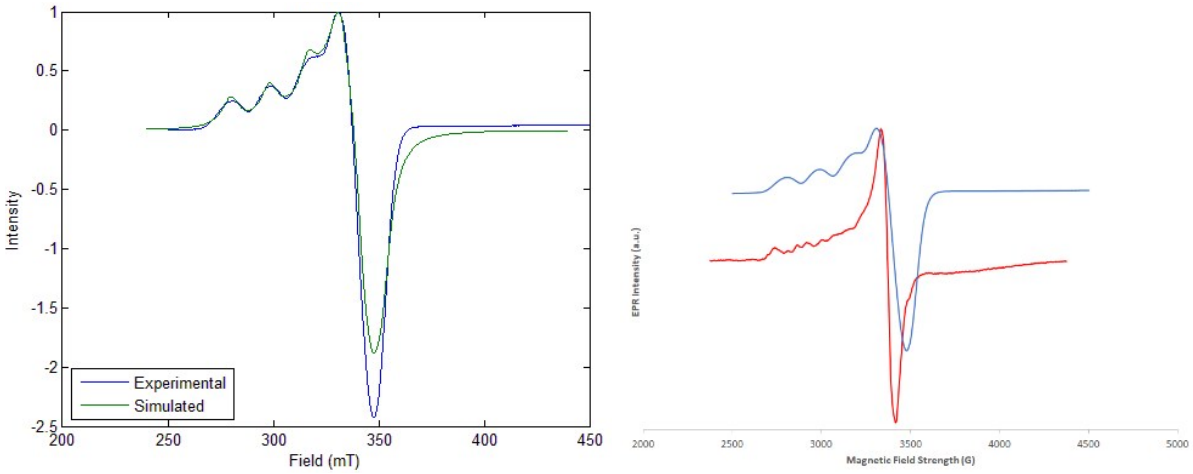

Figure S36. (left) Experimental (blue traces) and simulated (green traces) X-band EPR spectra for **10** at 9.383448 GHz and 5 K. (right) Overlay of EPR spectra in solid state (blue traces) and in ethanolic solution (red traces) for **10** at 9.383448 GHz and 5 K.

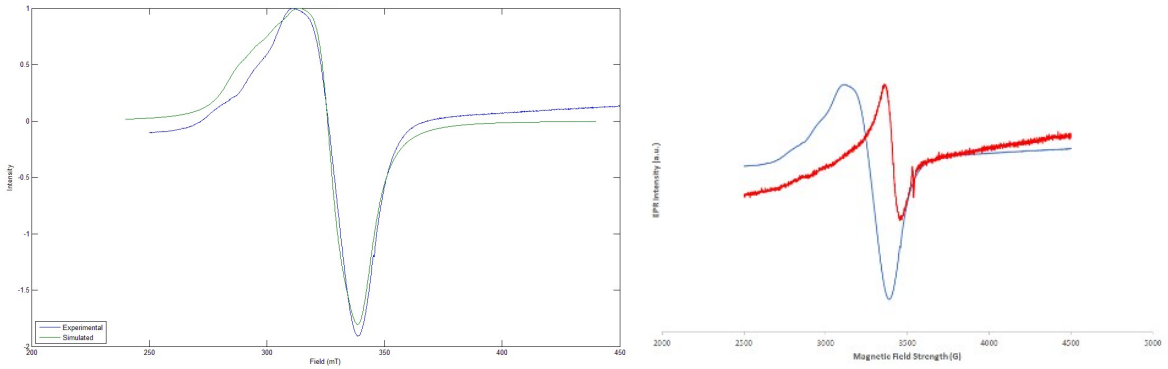

Figure S37. (left) Experimental (blue traces) and simulated (green traces) X-band EPR spectra for **12** at 9.303858 GHz and 5 K. (right) Overlay of EPR spectra in solid state (blue traces) and in methanolic solution (red traces) for **12** at 9.303858 GHz and 5 K.

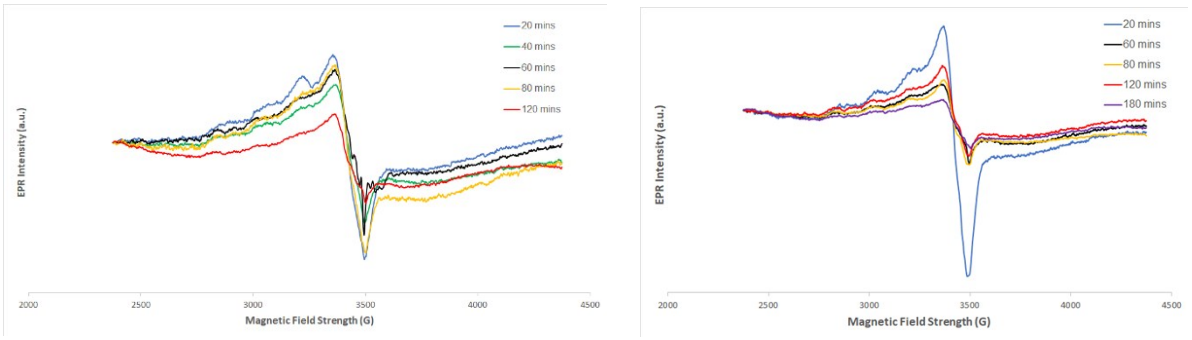

Figure S38. (left) Overlay of EPR spectra of aliquots from the catalytic reaction (**10** used as catalyst) during the synthesis of triazole **18aa** in selected times. (right) Overlay of EPR spectra of aliquots from the catalytic reaction (**10** used as catalyst), with 15% Sodium-L-ascorbate added, during the synthesis of triazole **18aa** in selected times.

Evaluation of catalytic conditions

Table S5. Evaluation of various Cu^{I} and Cu^{II} salts in the synthesis of triazole **18aa**.

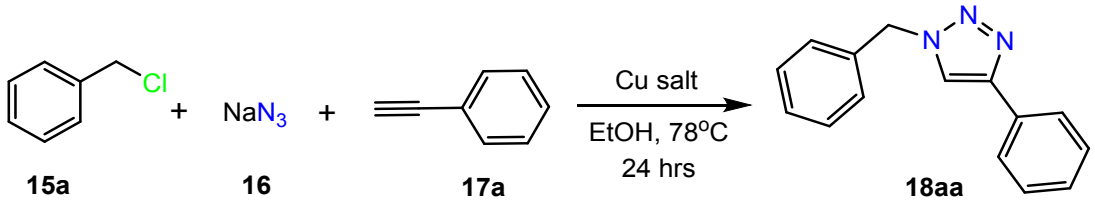

15a **16** **17a** **18aa**

Entry	Catalyst	Conversion (%)[a]	Yield (%)[b]	Regioselectivity	TON/TOF (hr^{-1})
1	$Cu^{I}Cl$	100	72	99:1	14.4/0.6
2	$Cu^{I}(BF_4)(MeCN)_4$	93	80	99:1	18/0.75
3	$Cu^{I}(OTf)(MeCN)_4$	100	78	99:1	15.6/0.65
4	$Cu^{II}Cl_2$	79	35	99:1	7/0.29
5	$Cu^{II}Br_2$	77	32	98:2	6.4/0.27
6	$Cu^{II}(OTf)_2 \cdot H_2O$	99	78	99:1	15.6/0.65
7	$Cu^{II}(OAc)_2 \cdot H_2O$	92	40	99:1	8/0.33
8	$Cu^{II}(ClO_4)_2 \cdot 6H_2O$	99	76	97:3	15.2/0.63
9	$Cu^{II}(BF_4)_2 \cdot 6H_2O$	99	71	96:4	14.2/0.59
10	$Cu^{II}(NO_3)_2 \cdot 2.5H_2O$	93	62	96:4	12.4/0.52

Reaction conditions: benzyl chloride (0.5 mmol), sodium azide (0.5 mmol), phenylacetylene (0.5 mmol), catalyst (5% mol), EtOH (3 mL), heated at 78°C for 24 h. [a]: based on benzyl chloride, [b]: calculated from the crude mixture by ^{1}HNMR. The reported[1] ^{1}HNMR peaks of the 1,5-analogue were employed to determine regioselectivity.

Characterization data of products (^{1}H, ^{13}CNMR and HRMS spectra)

1-benzyl-4-phenyl-1H-1,2,3-triazole (18aa)[2]

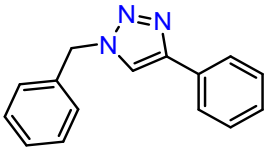

Yellow oil; ^{1}H NMR (500 MHz, $CDCl_3$) δ 7.81 (d, J = 7.7 Hz, 2H), 7.68 (s, 1H), 7.42 – 7.30 (m, 8H), 5.59 (s, 2H). ^{13}C NMR (126 MHz, $CDCl_3$) δ 134.46, 129.18, 128.86, 128.83, 128.32, 128.09, 125.75, 54.39. HRMS for $C_{15}H_{14}N_3$ [M + 1]: calc: 236.1182, found: 236.1174.

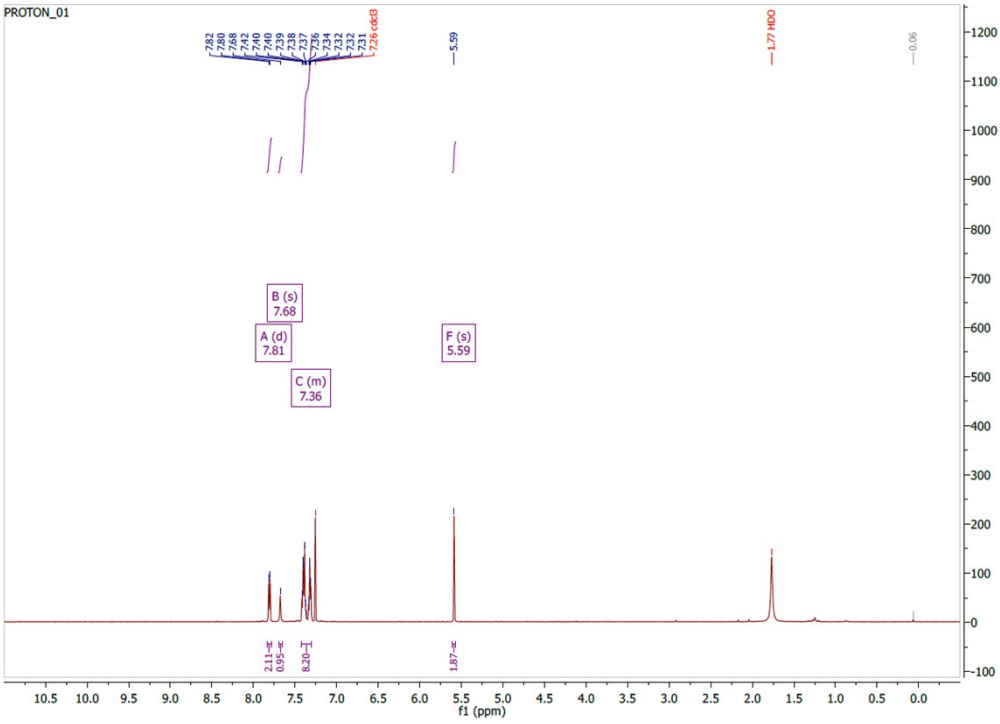

Figure S39. ^{1}H NMR spectrum of triazole **18aa**.

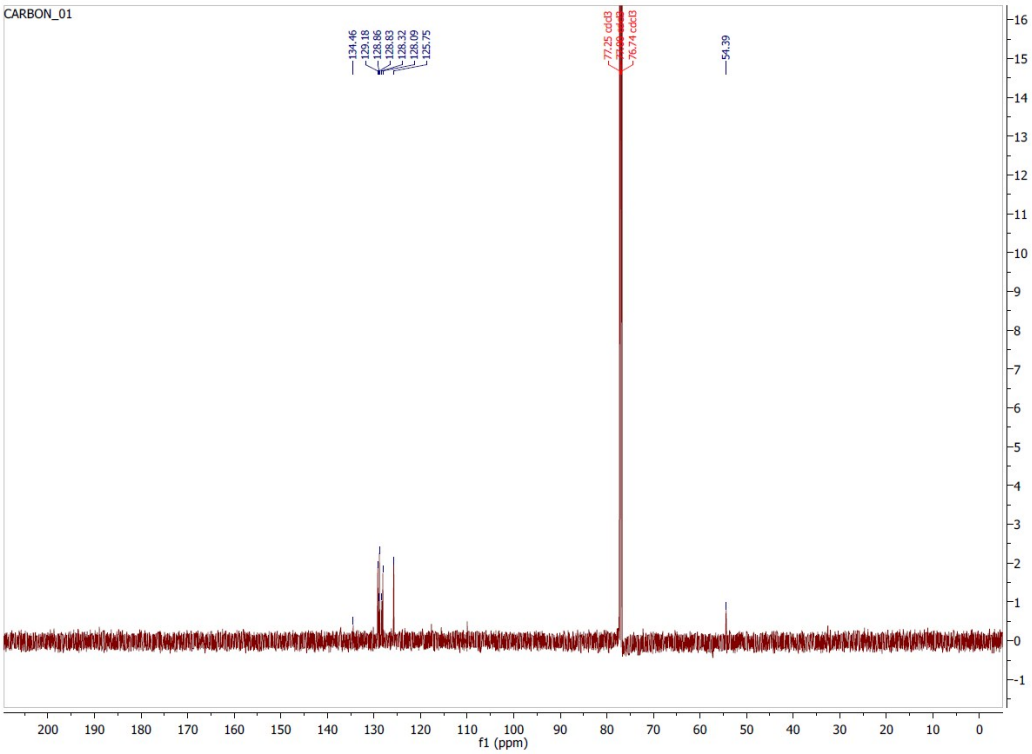

Figure S40. ^{13}C NMR spectrum of triazole **18aa**.

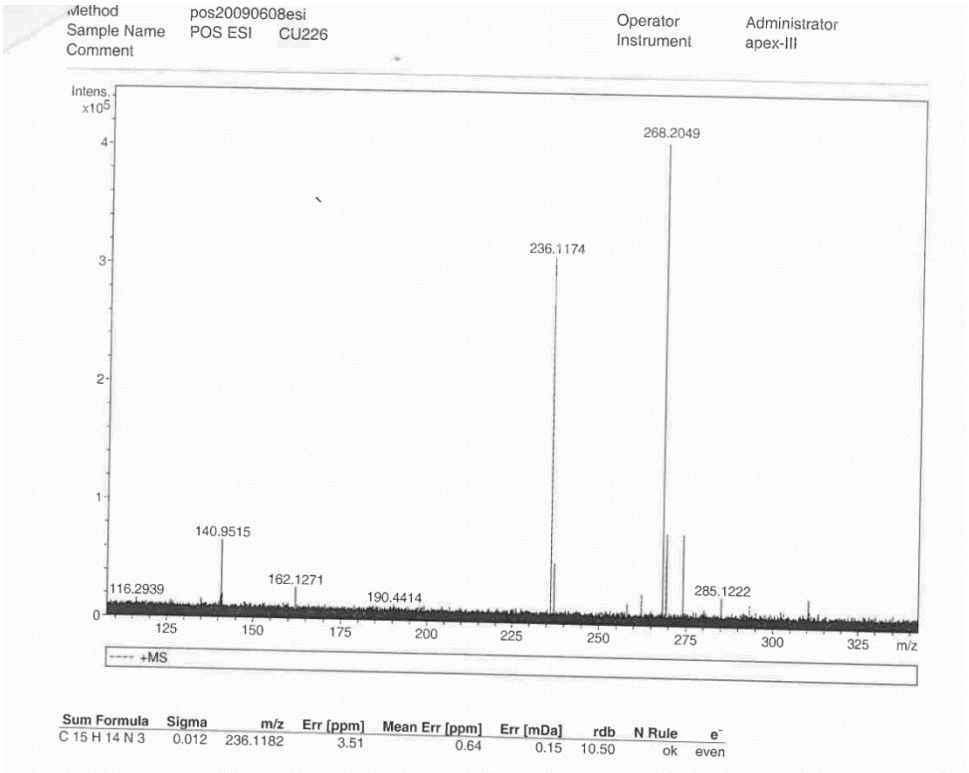

Figure S41. HRMS spectrum of triazole **18aa**.

1-benzyl-4-(4-methoxy)phenyl-1H-1,2,3-triazole (18ab)[2]

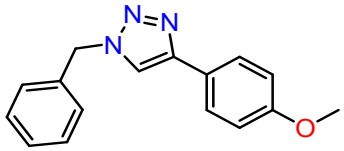

Yellow oil; ^{1}H NMR (500 MHz, $CDCl_3$) δ 7.75 – 7.69 (m, 2H), 7.58 (s, 1H), 7.40 – 7.34 (m, 3H), 7.30 (d, J = 7.0 Hz, 2H), 6.92 (d, J = 7.7 Hz, 2H), 5.56 (s, 2H), 3.82 (s, 3H). ^{13}C NMR (126 MHz, $CDCl_3$) δ 159.56, 148.05, 134.74, 129.12, 128.73, 128.03, 126.97, 123.25, 118.68, 114.17, 55.30, 54.20. HRMS for $C_{16}H_{16}N_3O$ [M + 1]: calc: 266.1288, found: 266.1279.

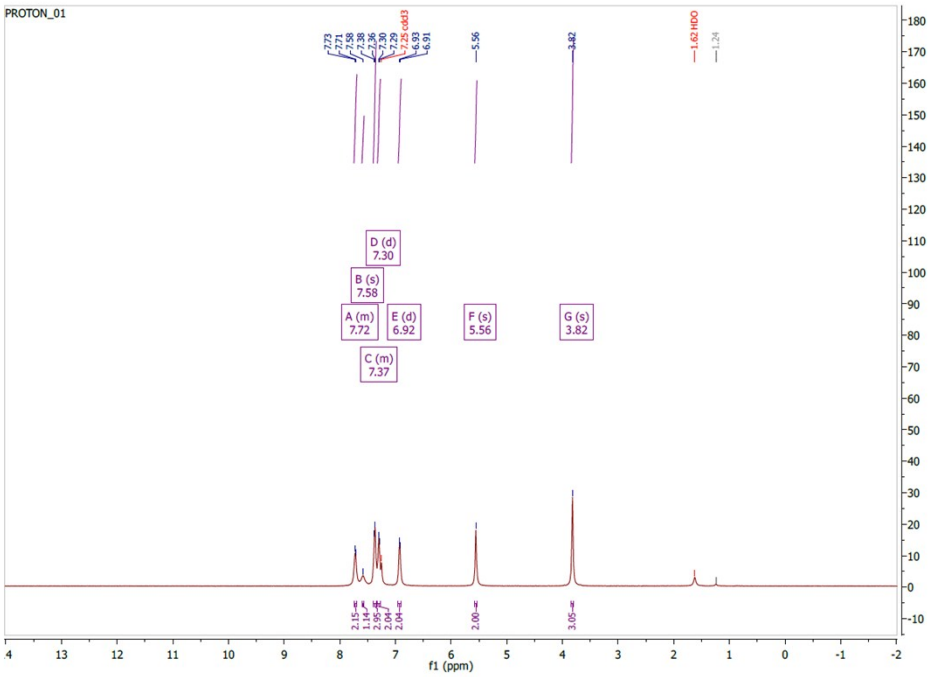

Figure S42. ^{1}H NMR spectrum of triazole **18ab**.

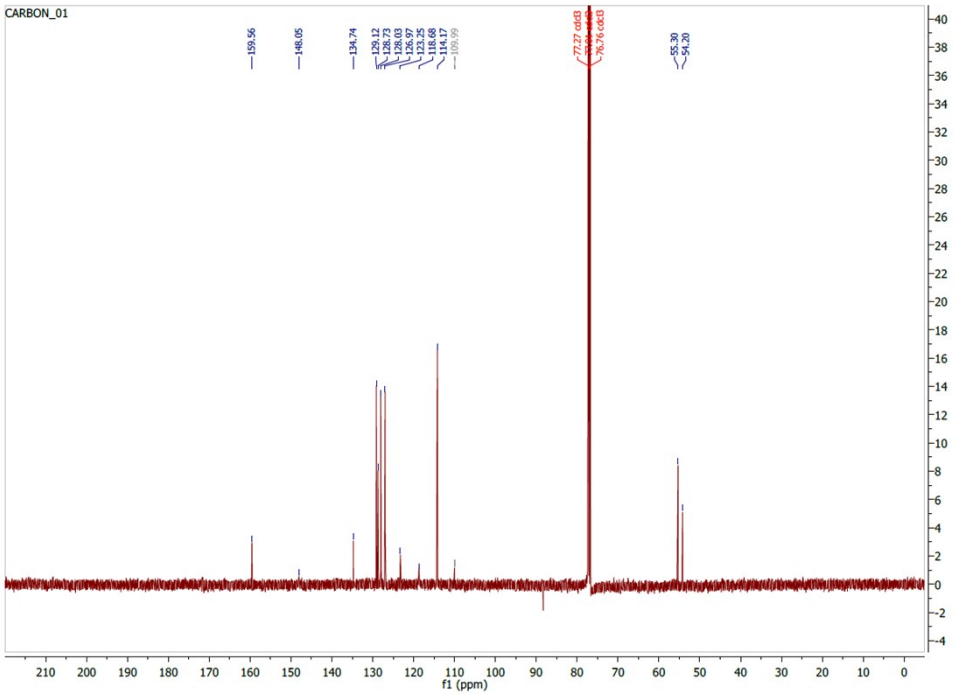

Figure S43. ^{13}C NMR spectrum of triazole **18ab**.

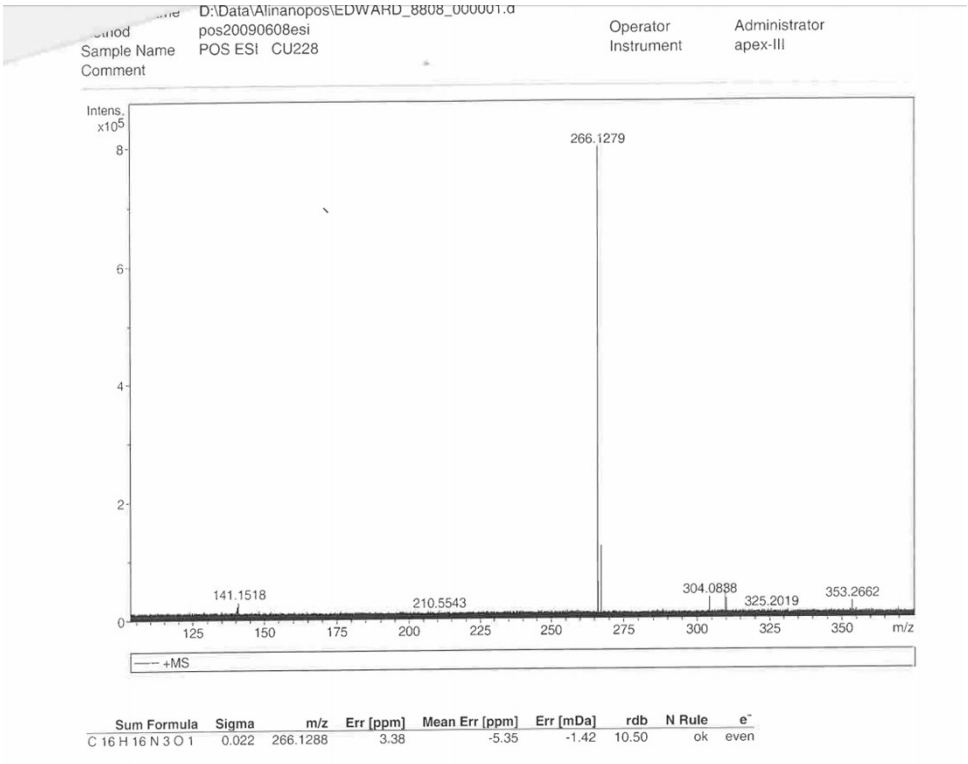

Figure S44. HRMS spectrum of triazole **18ab**.

1-benzyl-4-butyl-1H-1,2,3-triazole (18ac)[2]

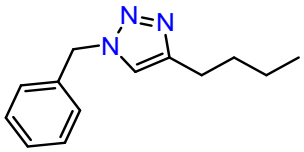

Yellow oil; ^{1}H NMR (600 MHz, $CDCl_3$) δ 7.37 – 7.28 (m, 3H), 7.23 – 7.20 (m, 2H), 7.19 (s, 1H), 5.44 (s, 2H), 2.66 (t, *J* = 7.8 Hz, 2H), 1.60 (p, *J* = 7.7 Hz, 2H), 1.33 (q, *J* = 7.5 Hz, 2H), 0.88 (t, *J* = 7.4 Hz, 3H). ^{13}C NMR (151 MHz, $CDCl_3$) δ 148.83, 135.03, 128.97, 128.51, 127.89, 120.56, 53.88, 31.48, 25.37, 22.28, 13.77. HRMS for $C_{13}H_{18}N_3$ [M + 1]: calc: 216.1495, found: 216.1494.

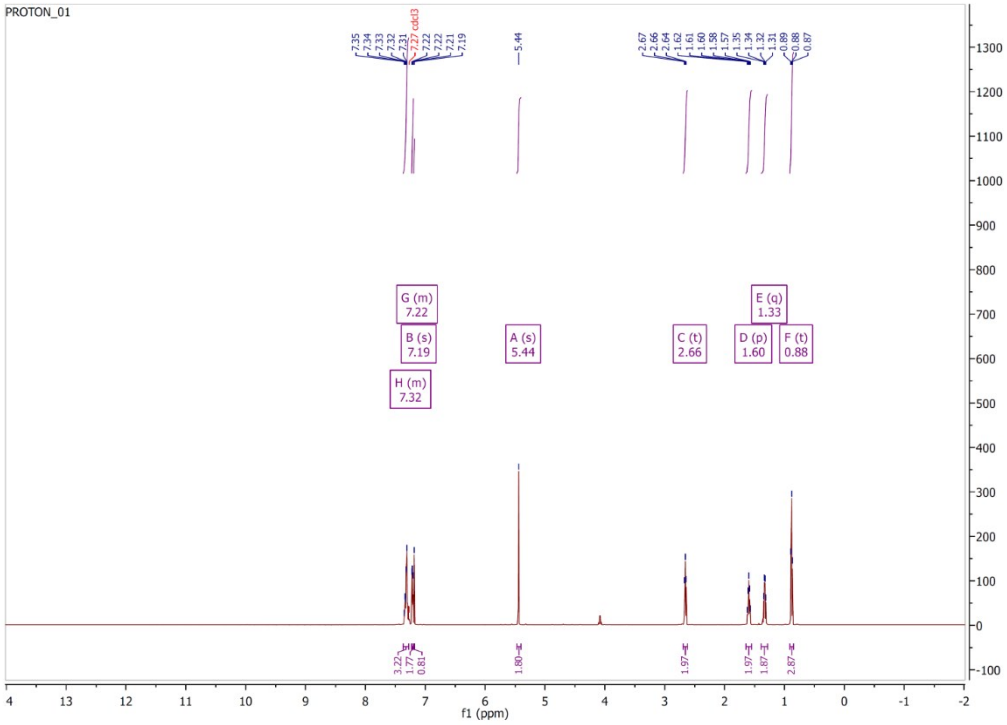

Figure S45. ^{1}H NMR spectrum of triazole **18ac**.

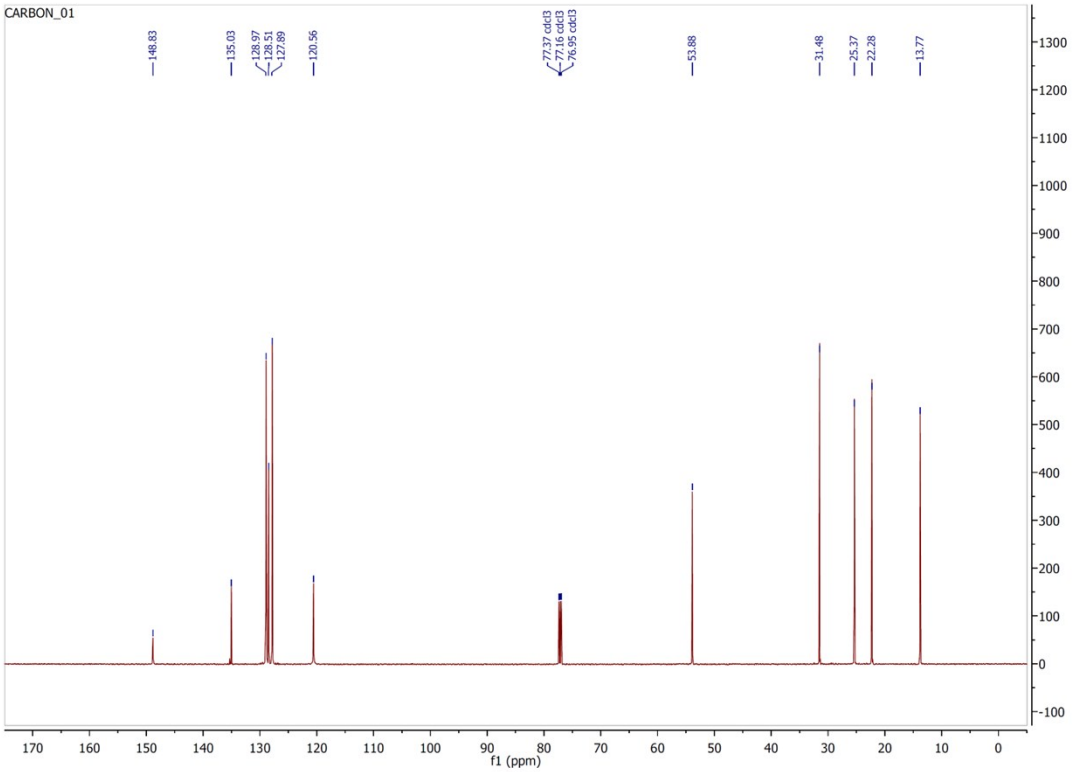

Figure S46. ^{13}C NMR spectrum of triazole **18ac**.

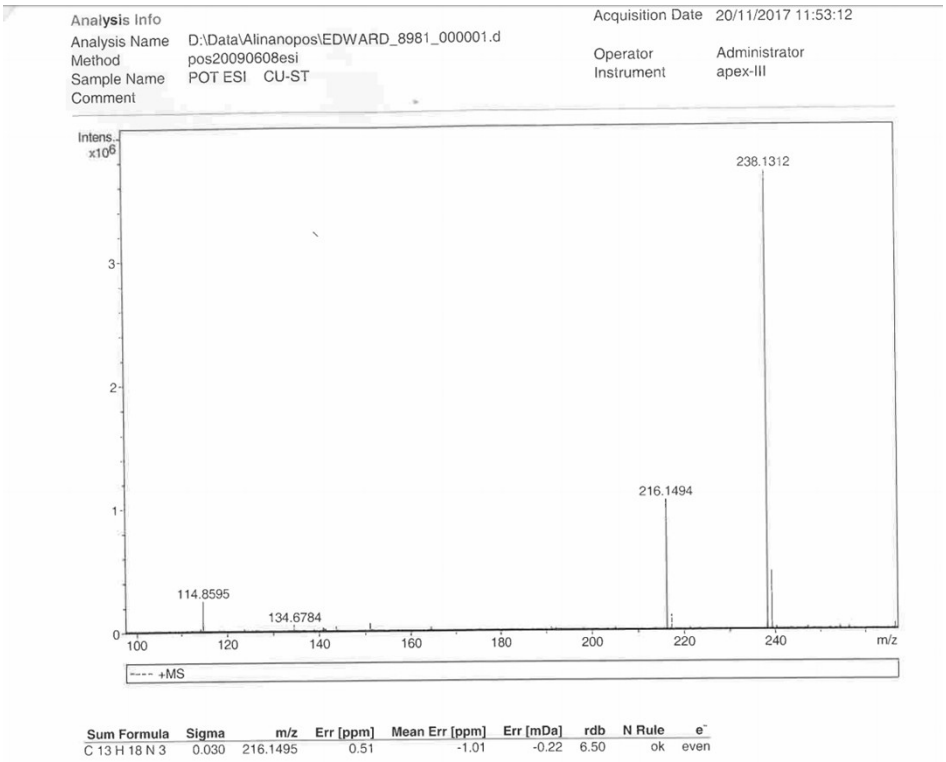

Figure S47. HRMS spectrum of triazole **18ac**.

(1-benzyl-1H-1,2,3-triazol-4-yl)methanol (18ad)[2]

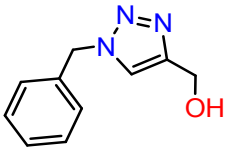

Yellow oil; ^{1}H NMR (600 MHz, $CDCl_3$) δ 7.48 (s, 1H), 7.38 – 7.30 (m, 3H), 7.29 – 7.22 (m, 2H), 5.48 (s, 2H), 4.72 (s, 2H). ^{13}C NMR (151 MHz, $CDCl_3$) δ 148.41, 134.47, 129.08, 128.75, 128.10, 122.15, 56.16, 54.20. HRMS for $C_{10}H_{12}N_3O$ [M + 1]: calc: 190.0975, found: 190.0968.

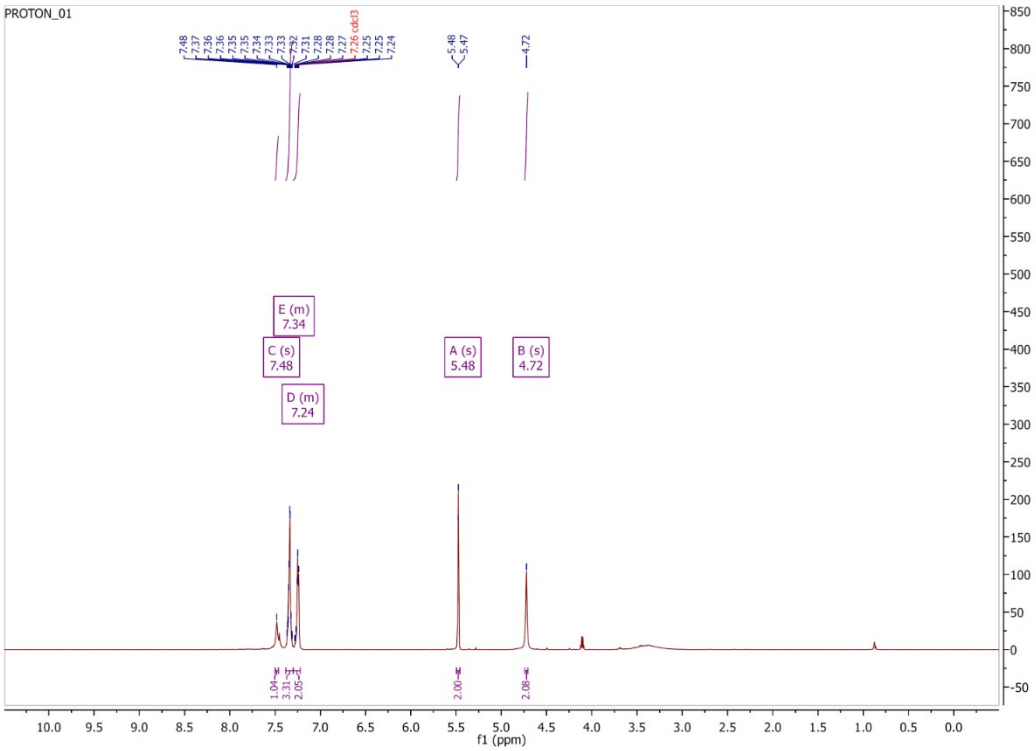

Figure S48. ^{1}H NMR spectrum of triazole **18ad**.

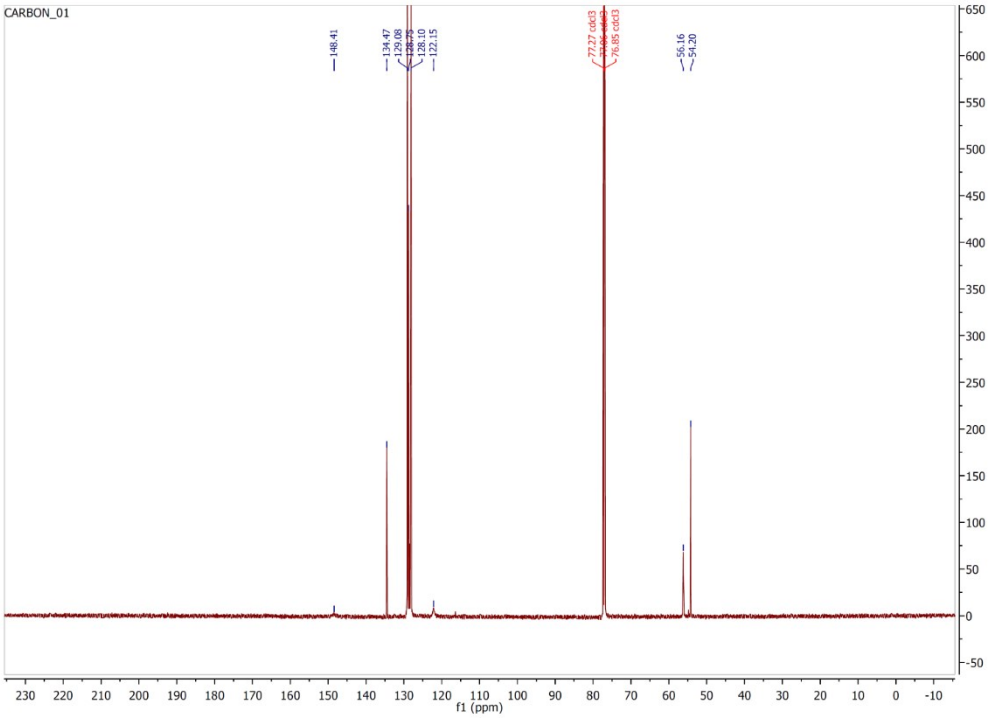

Figure S49. ^{13}C NMR spectrum of triazole **18ad**.

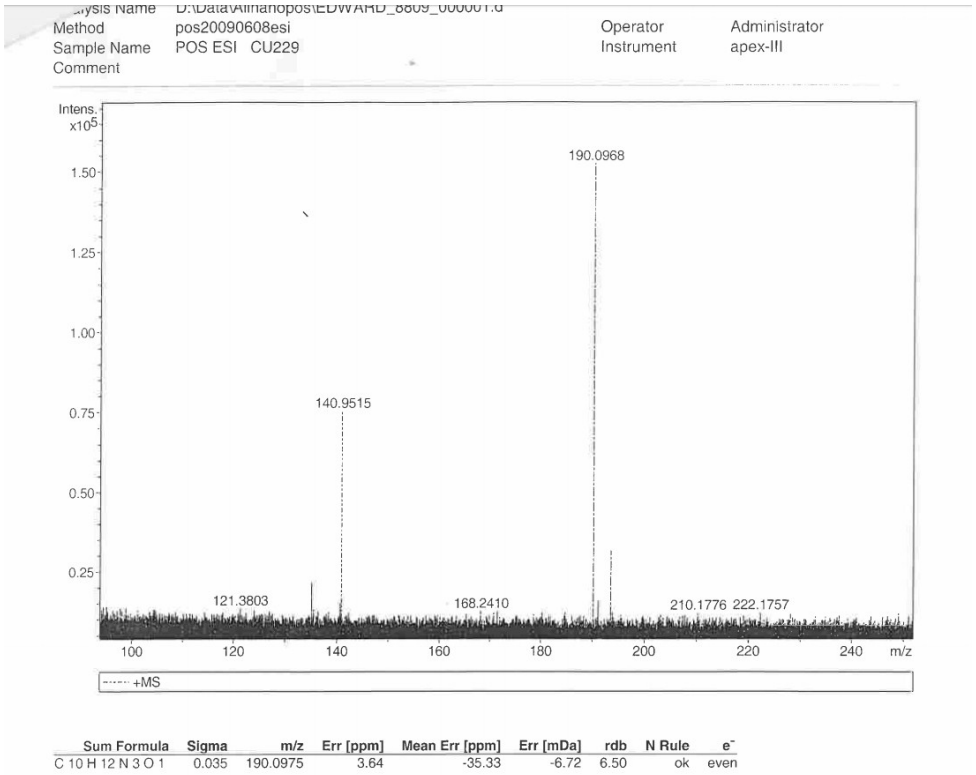

Sum Formula	Sigma	m/z	Err [ppm]	Mean Err [ppm]	Err [mDa]	rdb	N Rule	e⁻
C 10 H 12 N 3 O 1	0.035	190.0975	3.64	-35.33	-6.72	6.50	ok	even

Figure S50. HRMS spectrum of triazole **18ad**.

2-(1-benzyl-1H-1,2,3-triazol-4-yl)ethanol (18ae)[2]

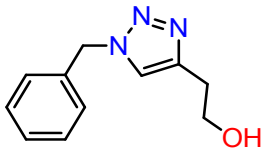

Yellow oil; ^{1}H NMR (600 MHz, $CDCl_3$) δ 7.38 – 7.30 (m, 4H), 7.27 – 7.23 (m, 2H), 5.48 (s, 2H), 3.91 (s, 2H), 2.90 (t, J = 6.1, 2.0 Hz, 2H). ^{13}C NMR (151 MHz, $CDCl_3$) δ 145.99, 134.66, 129.07, 128.70, 128.05, 121.51, 61.51, 54.09, 28.70. HRMS for $C_{11}H_{14}N_3O$ [M + 1]: calc: 204.1131, found: 204.1131.

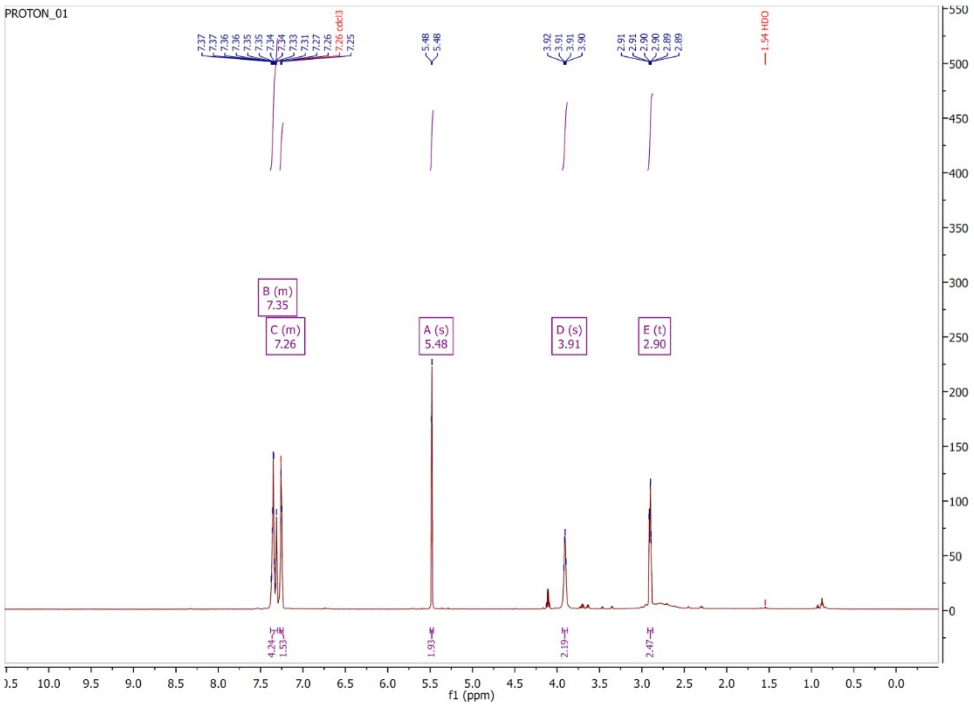

Figure S51. ^{1}H NMR spectrum of triazole **18ae**.

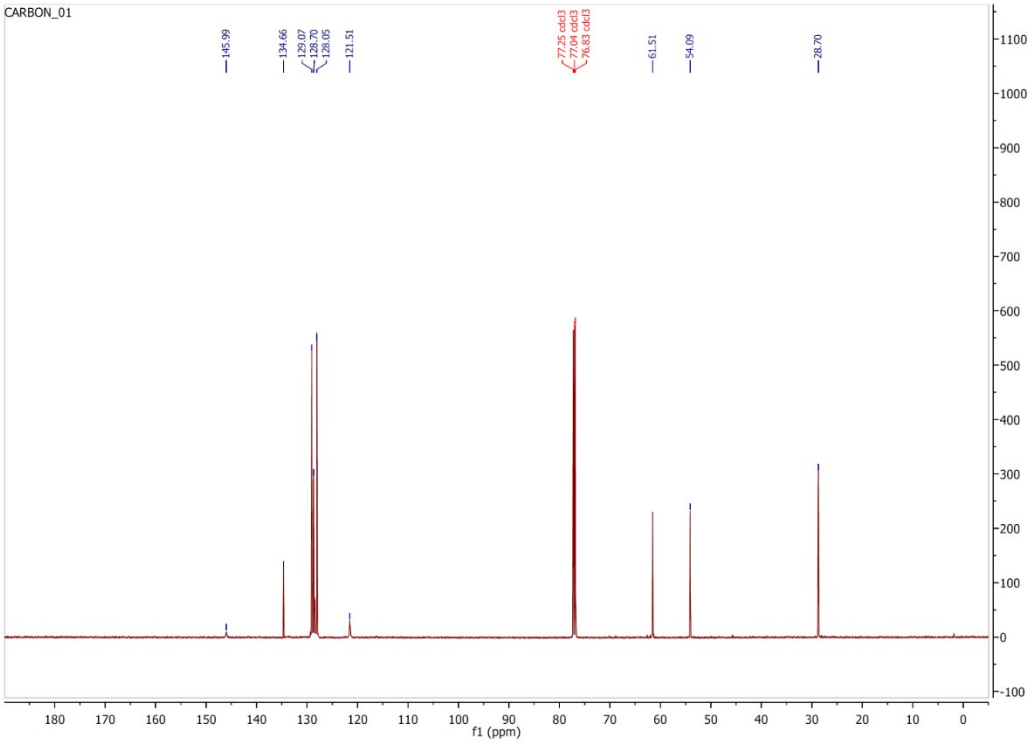

Figure S52. ^{13}C NMR spectrum of triazole **18ae**.

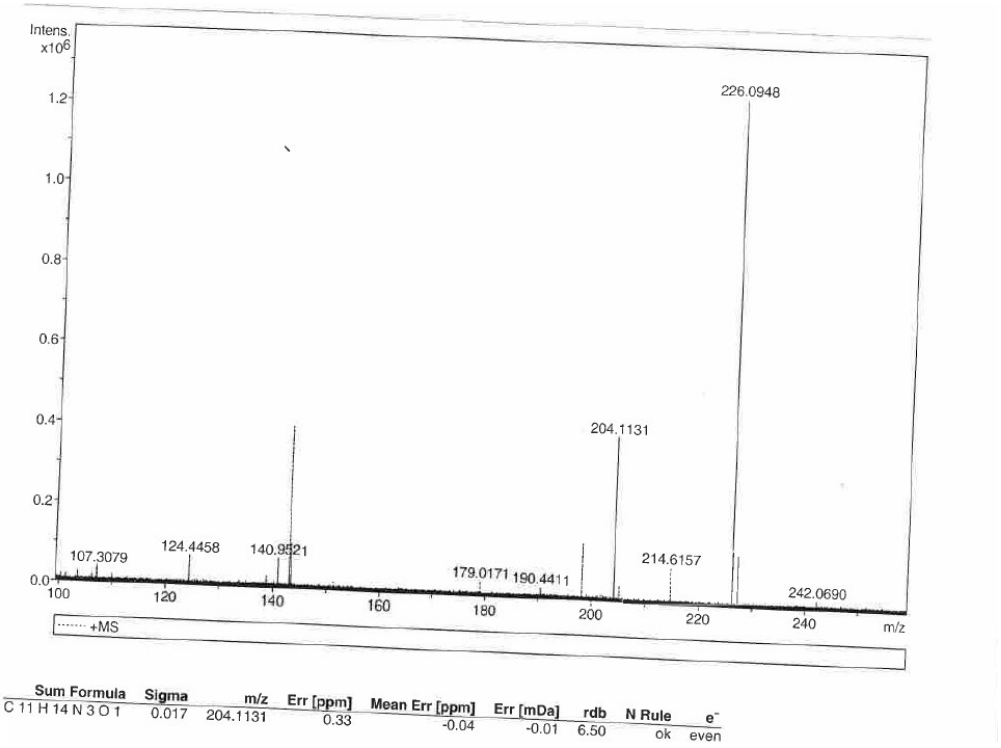

Figure S53. HRMS spectrum of triazole **18ae**.

Ethyl 1-benzyl-1H-1,2,3-triazole-4-carboxylate (18af)

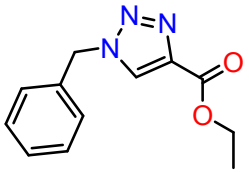

^{1}H NMR (600 MHz, $CDCl_3$) δ 7.97 (s, 1H), 7.31 – 7.27 (m, 3H), 7.23 – 7.17 (m, 2H), 5.58 (s, 2H), 4.40 (q, J = 7.2 Hz, 2H), 1.39 (t, J = 7.1 Hz, 3H). The found values match well to those in the literature.[2]

1-butyl-4-phenyl-1H-1,2,3-triazole (18ba)[3]

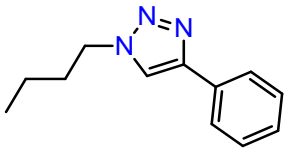

Yellow oil; ^{1}H NMR (500 MHz, $CDCl_3$) δ 7.84 (d, J = 7.6 Hz, 2H), 7.76 (s, 1H), 7.42 (t, J = 7.6 Hz, 2H), 7.33 (t, J = 7.4 Hz, 1H), 4.41 (t, J = 7.2 Hz, 2H), 1.99 – 1.89 (m, 2H), 1.45 – 1.34 (m, 2H), 0.97 (t, J = 7.4 Hz, 3H). ^{13}C NMR (126 MHz, $CDCl_3$) δ 148.58, 130.66, 128.81, 128.08, 125.67, 119.39, 50.16, 32.31, 19.72, 13.48. HRMS for $C_{12}H_{16}N_3$ [M + 1]: calc: 202.1339, found: 202.1341.

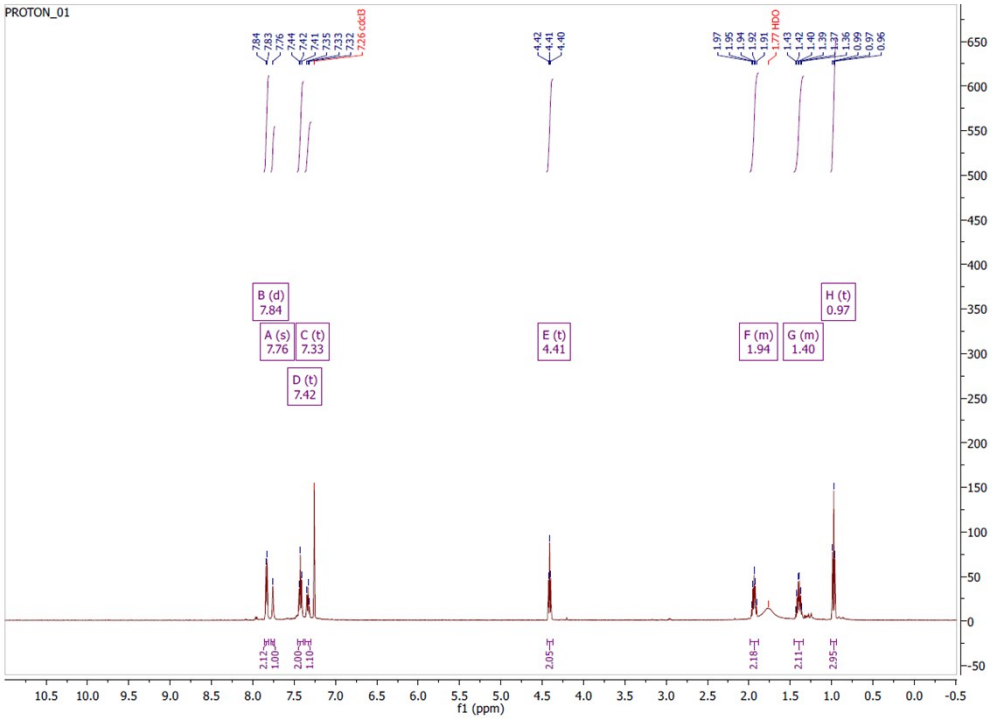

Figure S54. ^{1}H NMR spectrum of triazole **18ba**.

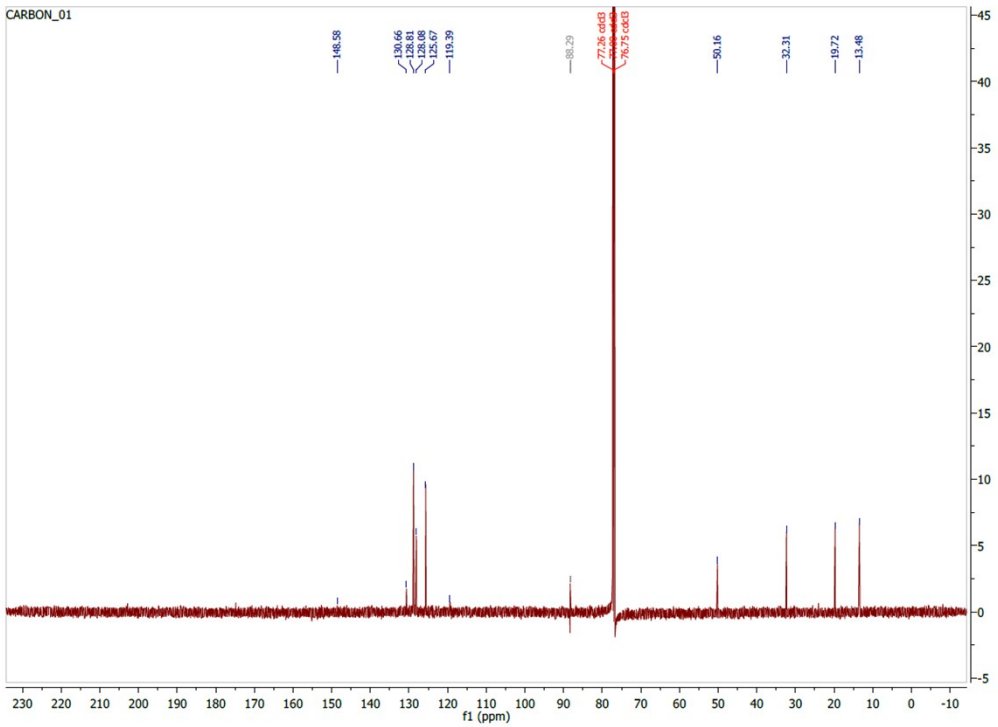

Figure S55. ^{13}C NMR spectrum of triazole **18ba**.

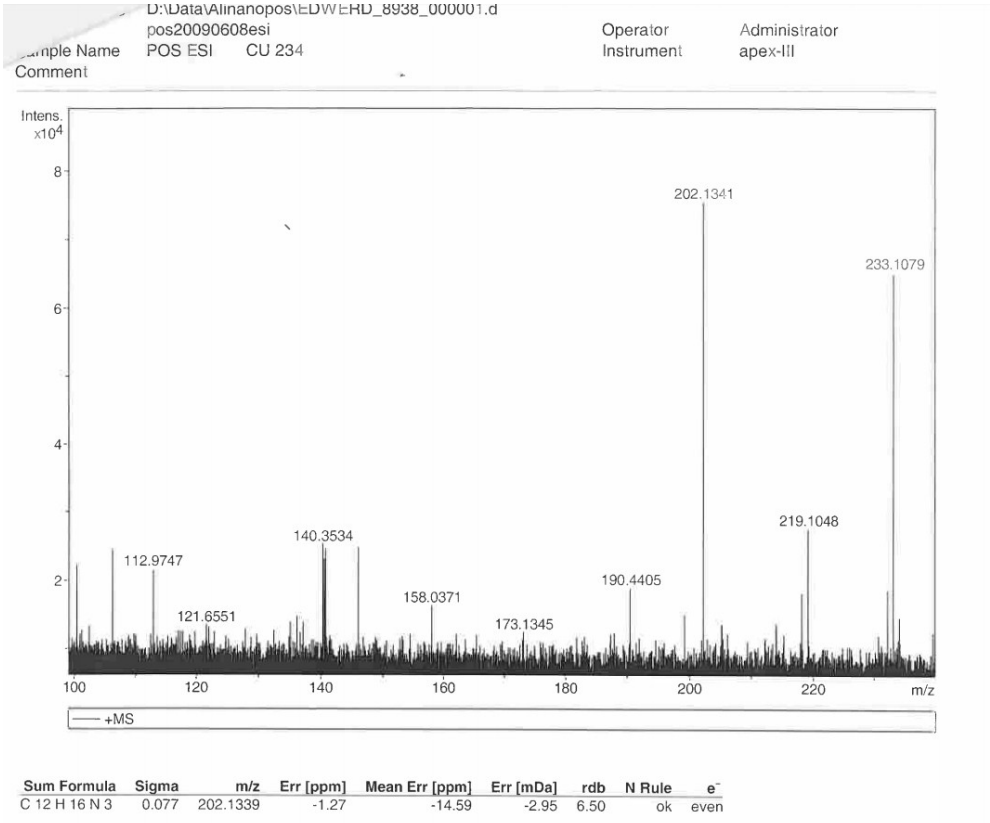

Sum Formula	Sigma	m/z	Err [ppm]	Mean Err [ppm]	Err [mDa]	rdb	N Rule	e⁻
C 12 H 16 N 3	0.077	202.1339	-1.27	-14.59	-2.95	6.50	ok	even

Figure S56. HRMS spectrum of triazole **18ba**.

1-butyl-4-(4-methoxy-phenyl)-1H-1,2,3-triazole (18bb)[3]

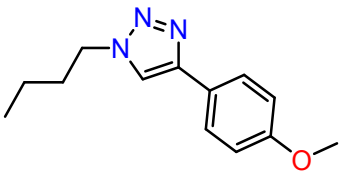

Yellow oil; ^{1}H NMR (500 MHz, $CDCl_3$) δ 7.76 (d, J = 8.3 Hz, 2H), 7.66 (s, 1H), 6.96 (d, J = 8.3 Hz, 2H), 4.40 (t, J = 7.3 Hz, 2H), 3.85 (s, 3H), 1.97 – 1.90 (m, 2H), 1.44 – 1.36 (m, 2H), 0.98 (t, J = 7.4 Hz, 3H). ^{13}C NMR (151 MHz, $CDCl_3$) δ 159.56, 150.61, 133.56, 126.99, 118.61, 114.23, 77.20, 76.99, 76.77, 55.32, 50.12, 32.30, 19.72, 13.46. HRMS for $C_{13}H_{18}N_3O$ [M + 1]: calc: 232.1444, found: 232.1447.

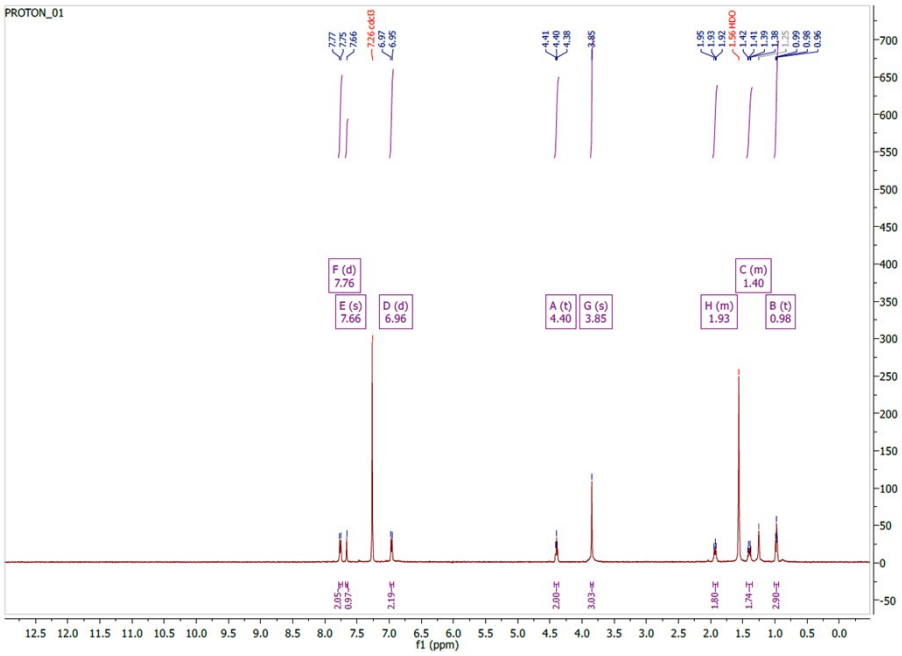

Figure S57. ^{1}H NMR spectrum of triazole **18bb**.

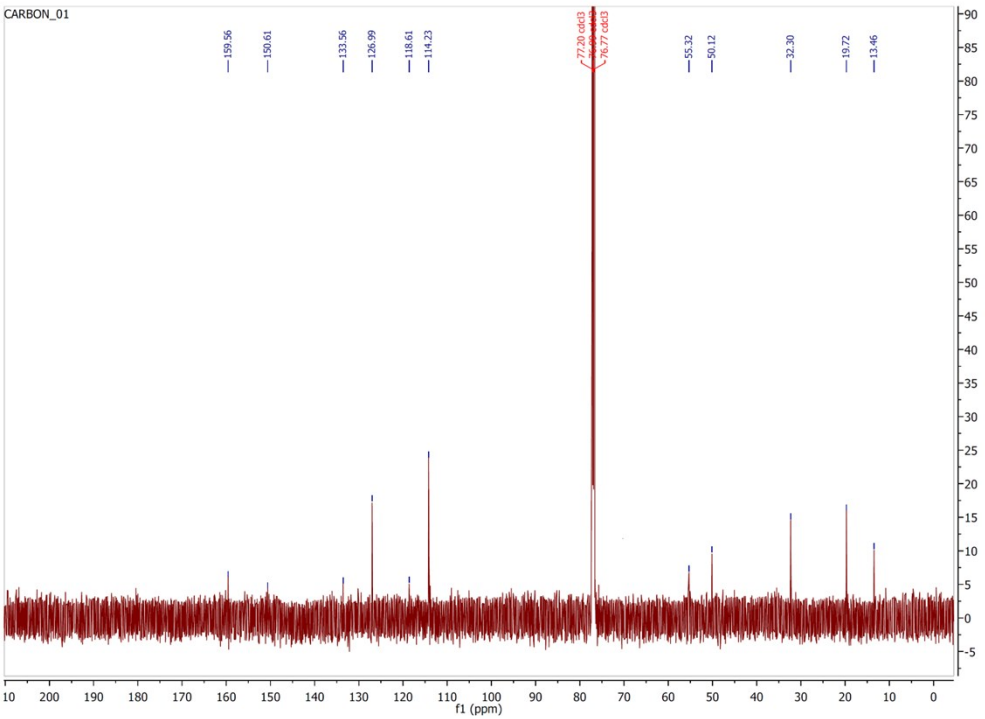

Figure S58. ^{13}C NMR spectrum of triazole **18bb**.

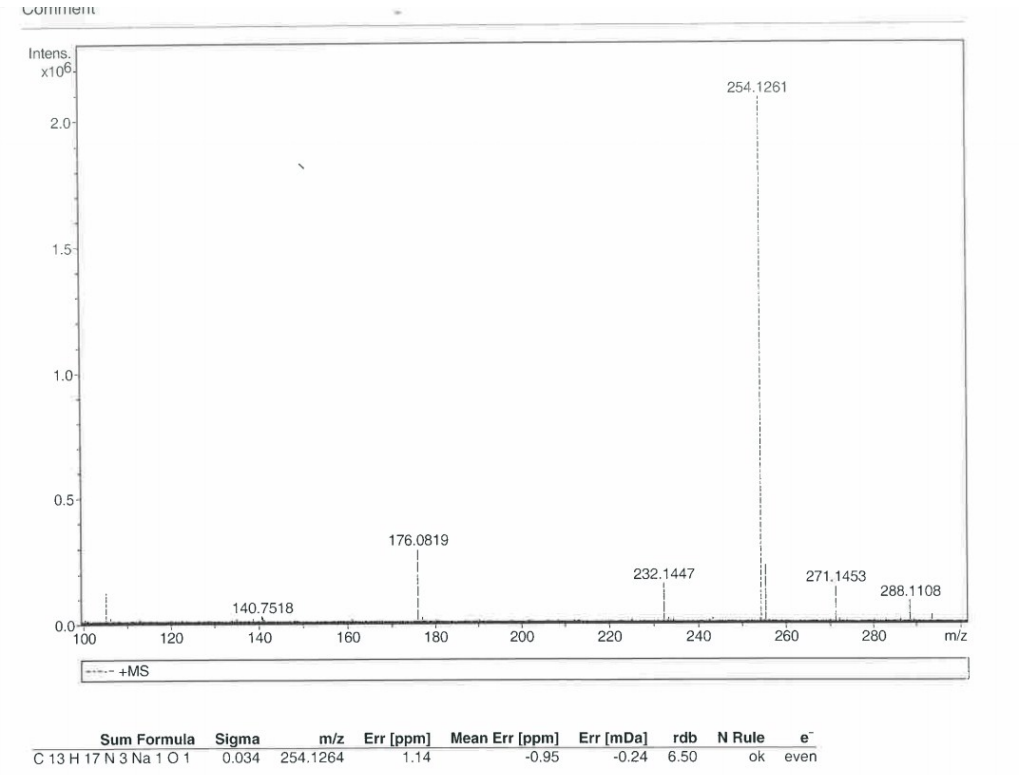

Sum Formula	Sigma	m/z	Err [ppm]	Mean Err [ppm]	Err [mDa]	rdb	N Rule	e⁻
C 13 H 17 N 3 Na 1 O 1	0.034	254.1264	1.14	-0.95	-0.24	6.50	ok	even

Figure S59. HRMS spectrum of triazole **18bb**.

1,4-dibutyl-1H-1,2,3-triazole (18bc)[4]

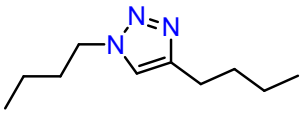

Yellow oil; ^{1}H NMR (500 MHz, $CDCl_3$) δ 7.27 (s, 1H), 4.32 (t, *J* = 7.2 Hz, 2H), 2.71 (t, *J* = 7.7 Hz, 2H), 1.91 – 1.83 (m, 2H), 1.69 – 1.61 (m, 2H), 1.43 – 1.30 (m, 4H), 1.00 – 0.89 (m, 6H). ^{13}C NMR (126 MHz, $CDCl_3$) δ 148.32, 120.41, 49.91, 32.31, 31.58, 25.35, 22.31, 19.72, 13.82, 13.47. HRMS for $C_{10}H_{20}N_3$ [M + 1]: calc: 182.1652, found: 182.1652.

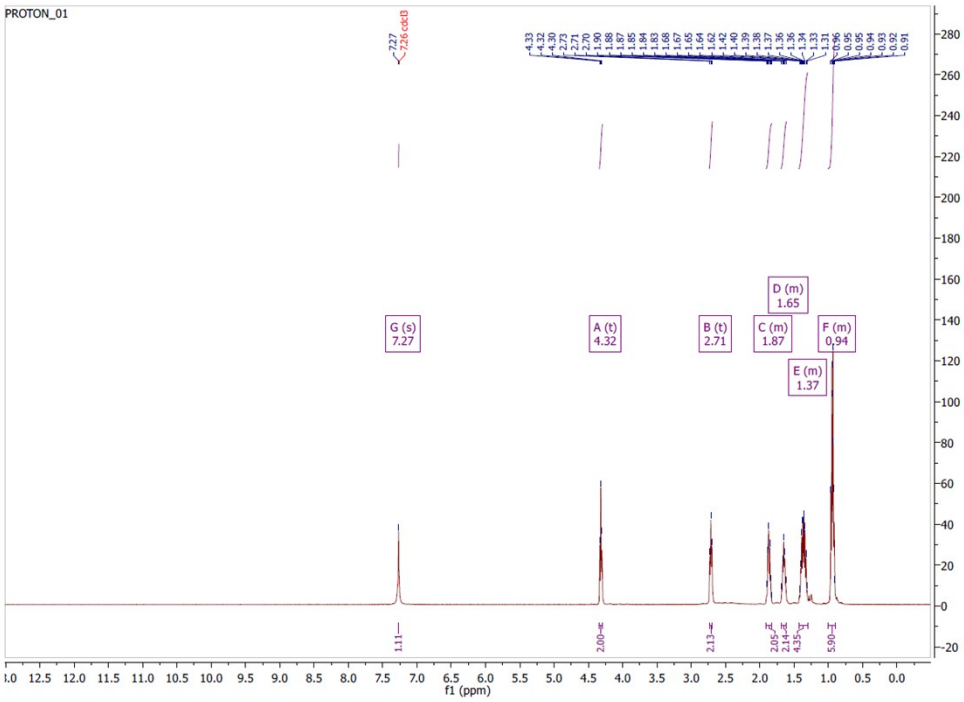

Figure S60. ^{1}H NMR spectrum of triazole **18bc**.

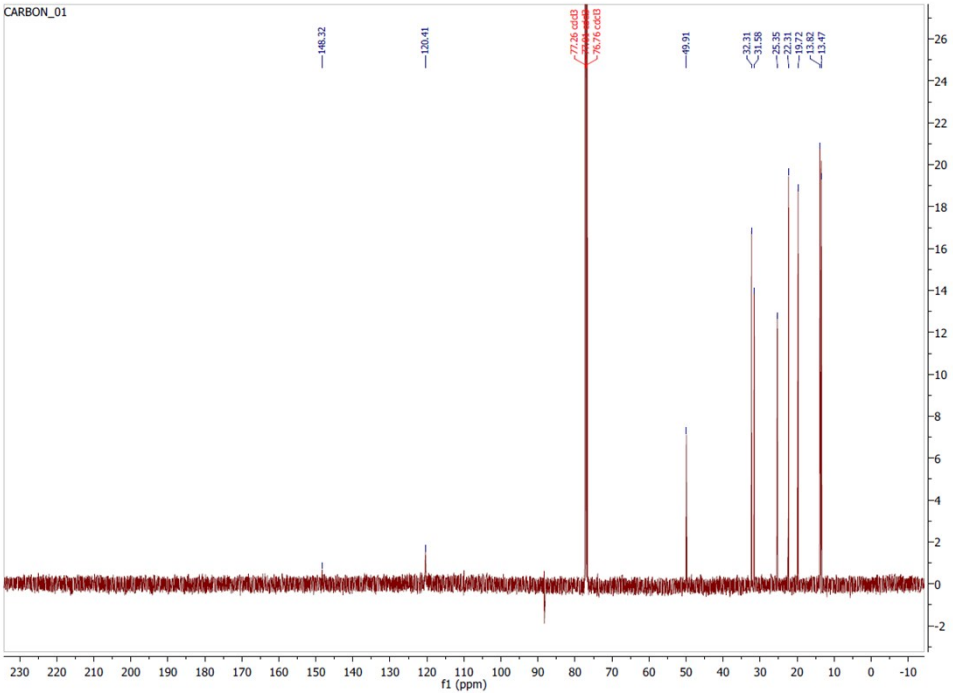

Figure S61. ^{13}C NMR spectrum of triazole **18bc**.

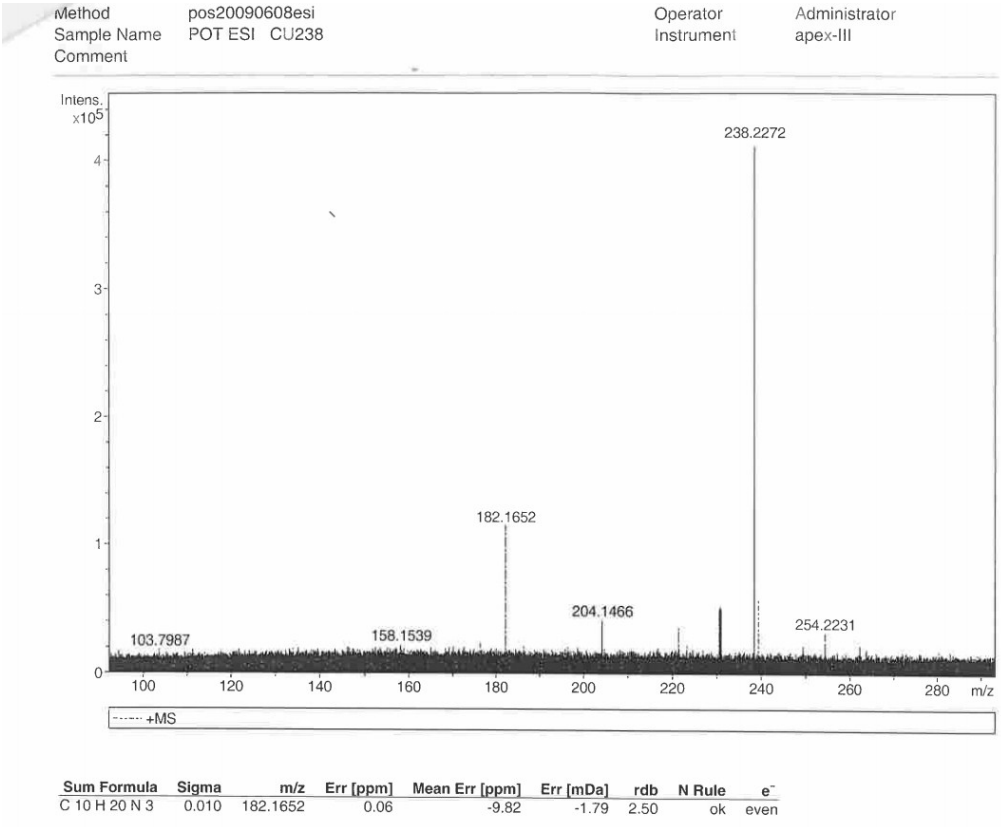

Figure S62. HRMS spectrum of triazole **18bc**.

(1-Butyl-1H-1,2,3-triazol-4-yl)methanol (18bd)[5]

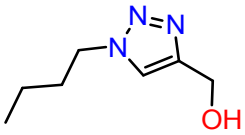

Light yellow oil; ^{1}H NMR (500 MHz, $CDCl_3$) δ 7.54 (s, 1H), 4.80 (s, 2H), 4.36 (t, J = 7.2 Hz, 2H), 1.89 (p, J = 7.5 Hz, 2H), 1.42 – 1.26 (m, 2H), 0.95 (t, J = 7.4 Hz, 3H). ^{13}C NMR (126 MHz, $CDCl_3$) δ 147.62, 121.66, 56.45, 50.14, 32.21, 19.67, 13.41. HRMS for $C_7H_{14}N_3O$ [M + 1]: calc: 156.1131, found: 156.1134

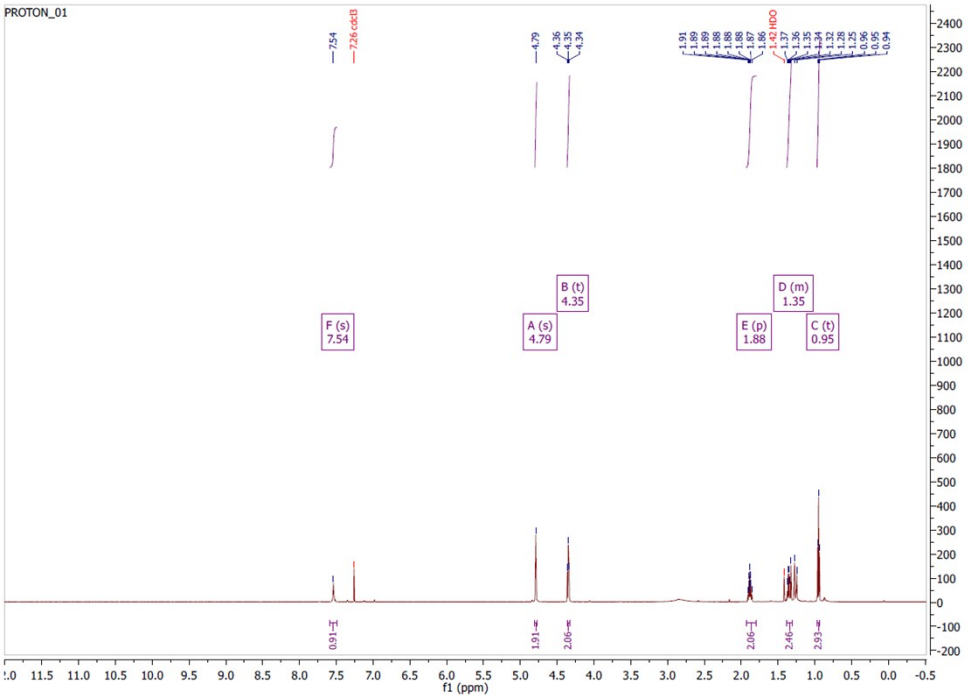

Figure S63. ^{1}H NMR spectrum of triazole **18bd**.

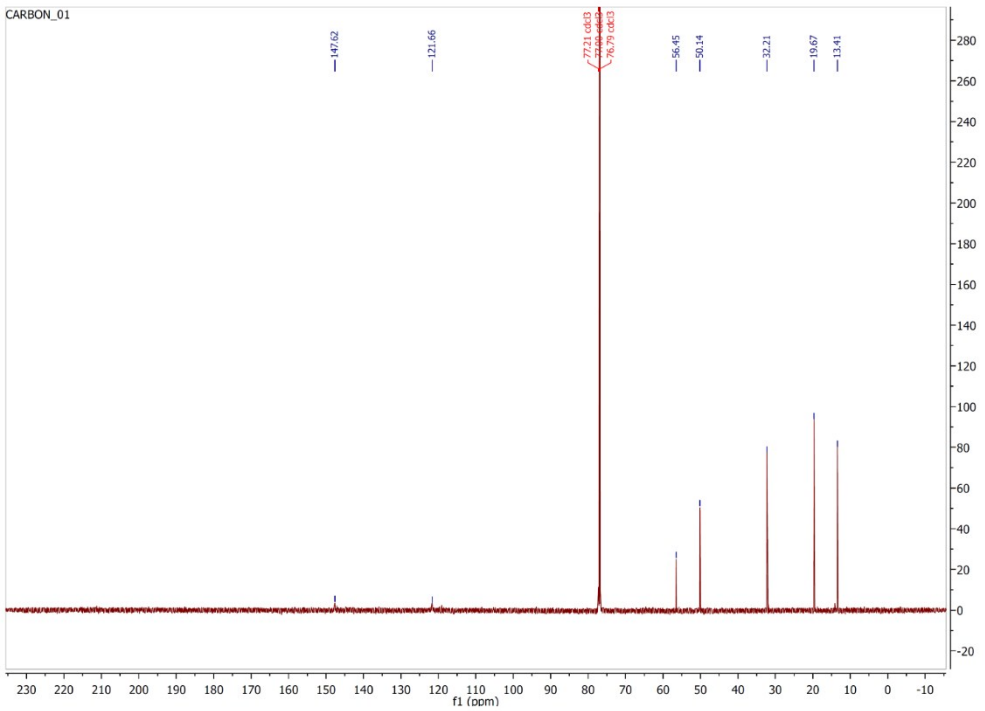

Figure S64. ^{13}C NMR spectrum of triazole **18bd**.

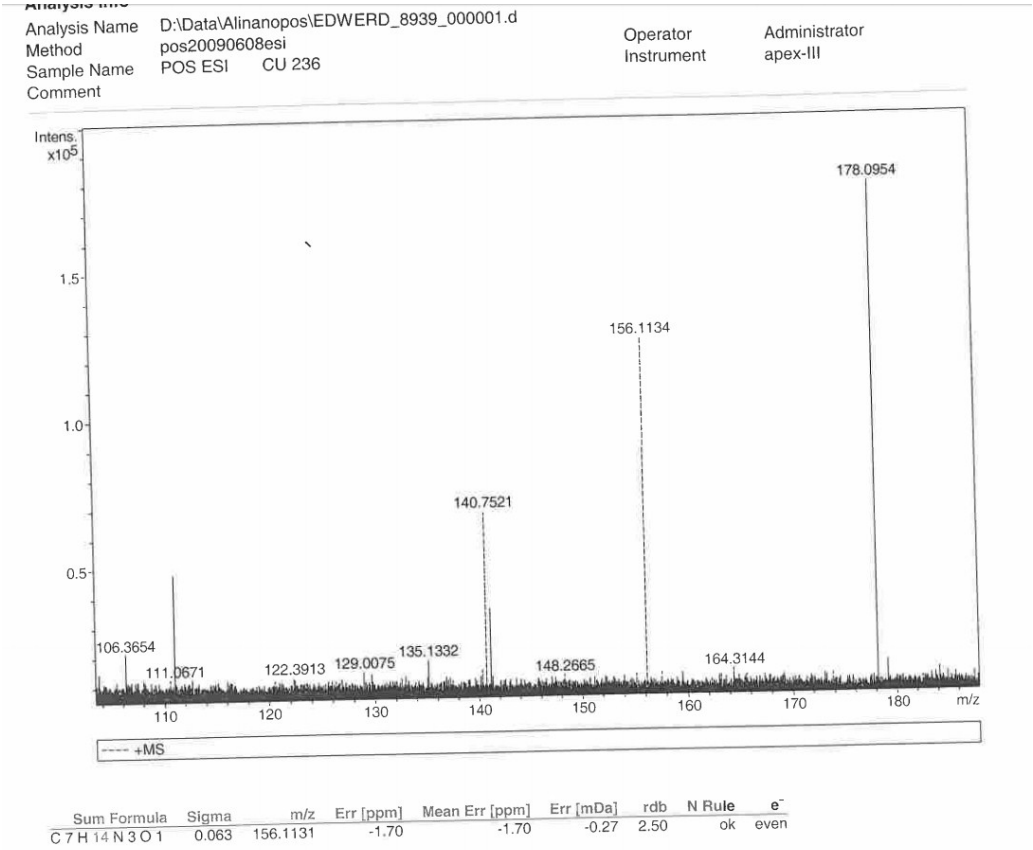

Figure S65. HRMS spectrum of triazole **18bd**.

2-(1-butyl-1H-1,2,3-triazol-4-yl)ethanol (18be)

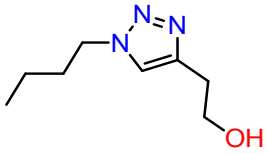

Light yellow oil; ^{1}H NMR (600 MHz, $CDCl_3$) δ 7.40 (s, 1H), 4.32 (t, *J* = 7.2 Hz, 2H), 3.96 (s, 2H), 2.93 (t, *J* = 5.7 Hz, 2H), 1.87 (p, *J* = 7.4 Hz, 2H), 1.38 – 1.24 (m, 2H), 0.95 (t, *J* = 7.3 Hz, 3H). ^{13}C NMR (126 MHz, $CDCl_3$) δ 147.06, 121.61, 61.64, 50.04, 32.21, 28.61, 19.70, 13.43. HRMS for $C_7H_{14}N_3O$ [M + 1]: calc: 170.1288, found: 170.1288.

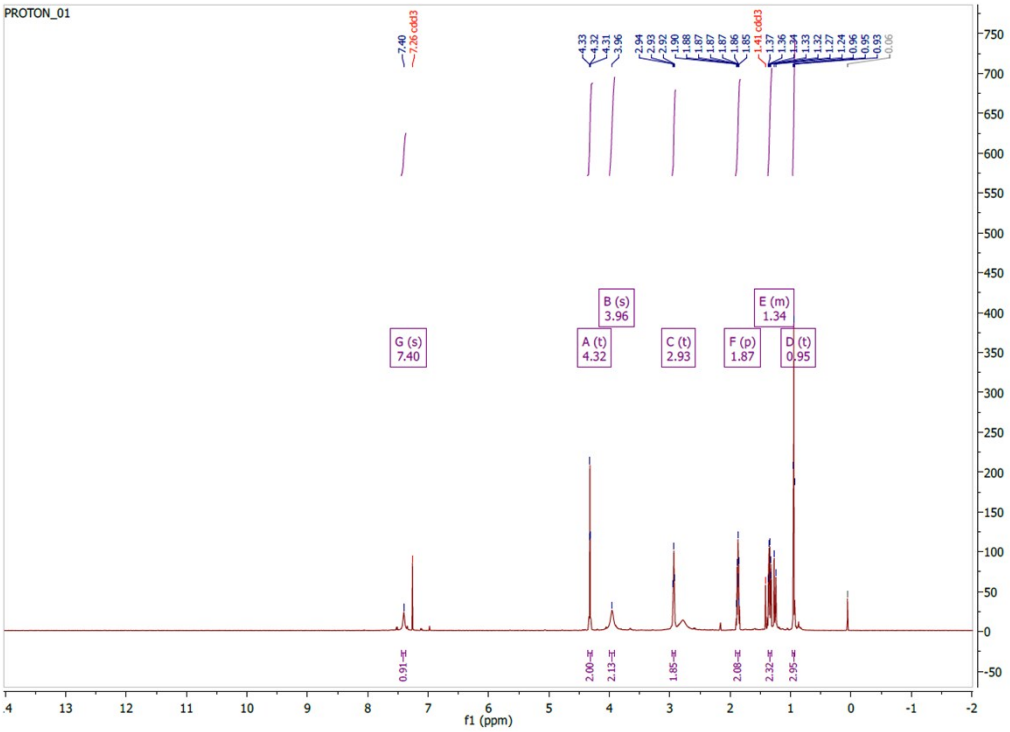

Figure S66. ^{1}H NMR spectrum of triazole **18be**.

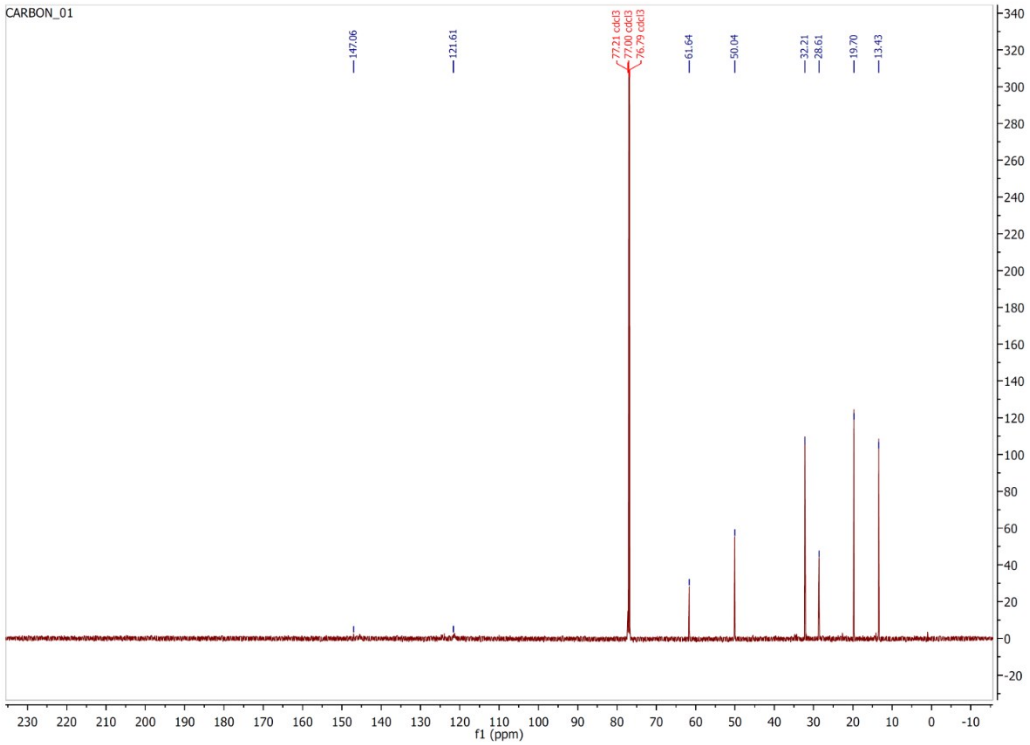

Figure S67. ^{13}C NMR spectrum of triazole **18be**.

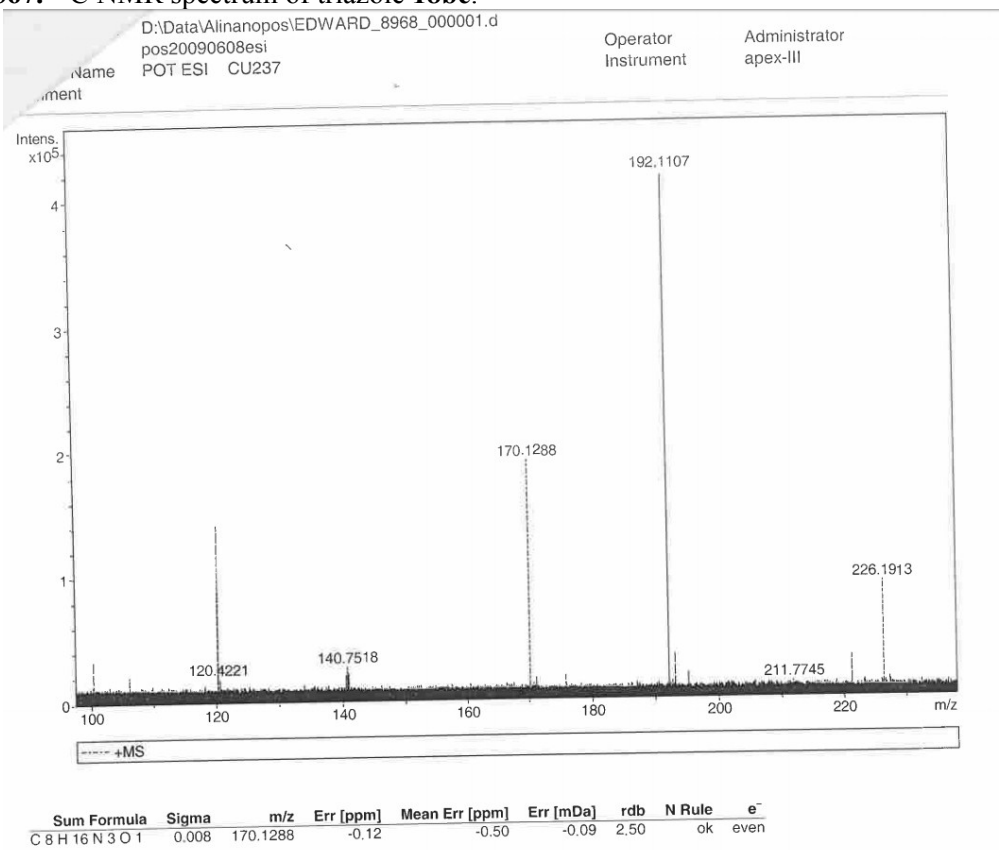

Sum Formula	Sigma	m/z	Err [ppm]	Mean Err [ppm]	Err [mDa]	rdb	N Rule	e⁻
C 8 H 16 N 3 O 1	0.008	170.1288	-0.12	-0.50	-0.09	2.50	ok	even

Figure S68. HRMS spectrum of triazole **18be**.

1,4-Diphenyl-1H-[1,2,3]-triazole (18ca)[6]

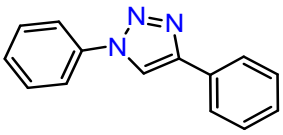

Yellow oil; ^{1}H NMR (600 MHz, $CDCl_3$) δ 8.20 (s, 1H), 7.92 (d, *J* = 7.4 Hz, 2H), 7.80 (d, *J* = 7.6 Hz, 2H), 7.55 (t, *J* = 7.6 Hz, 2H), 7.49 – 7.43 (m, 3H), 7.40 – 7.34 (m, 1H). ^{13}C NMR (151 MHz, $CDCl_3$) δ 148.39, 137.06, 130.23, 129.76, 128.90, 128.75, 128.40, 125.84, 120.51, 117.57, 77.21, 77.00, 76.79. HRMS for $C_{14}H_{12}N_3$ [M + 1]: calc: 222.1026, found: 222.1026.

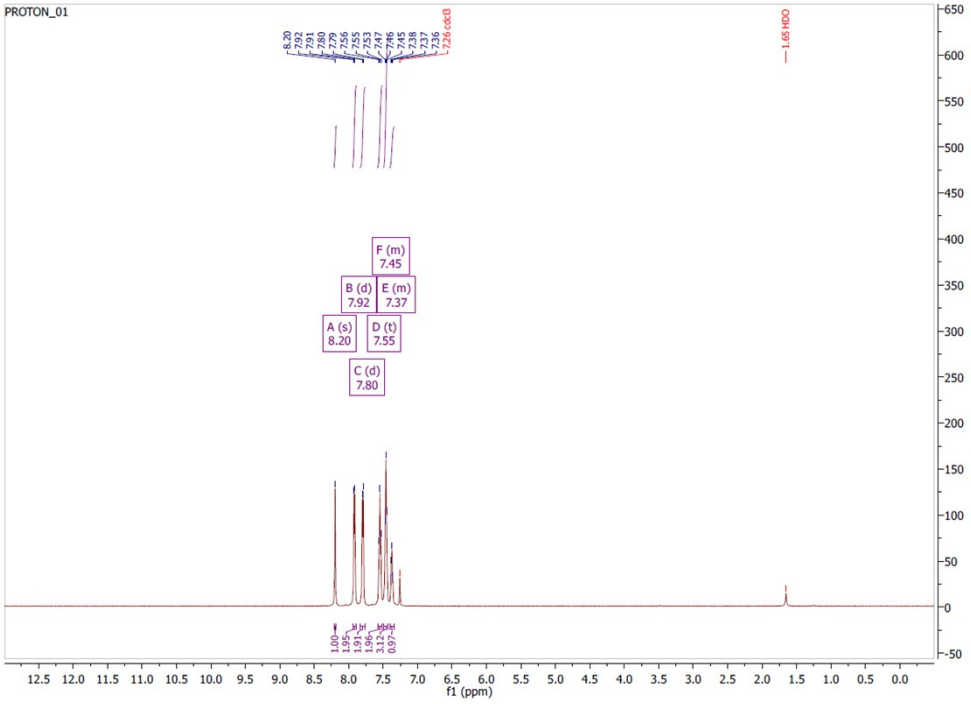

Figure S69. ^{1}H NMR spectrum of triazole **18ca**.

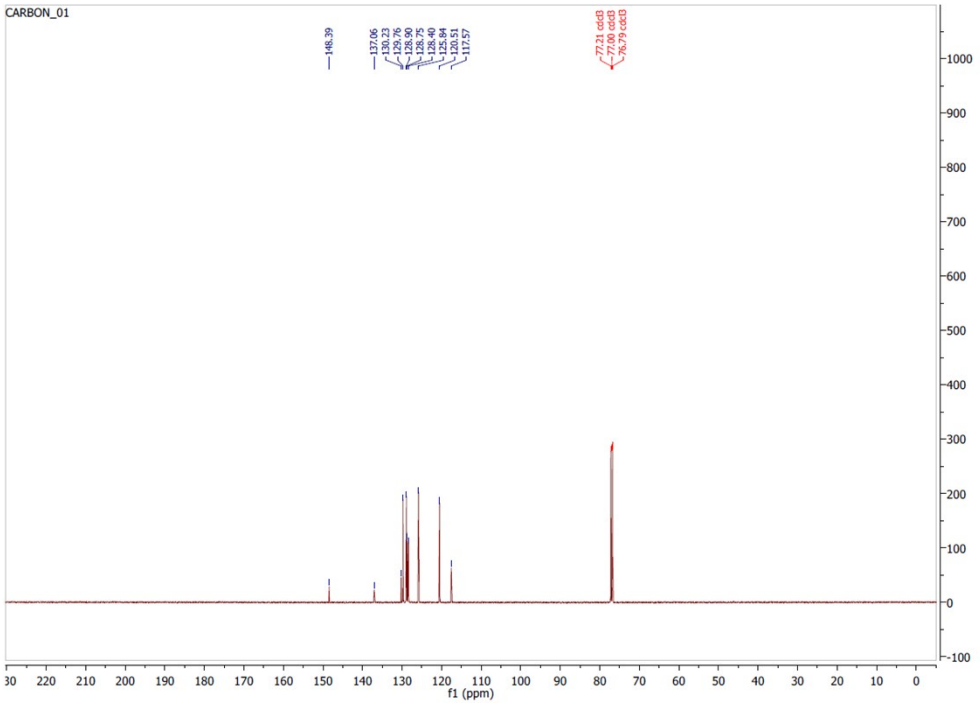

Figure S70. ^{13}C NMR spectrum of triazole **18ca**.

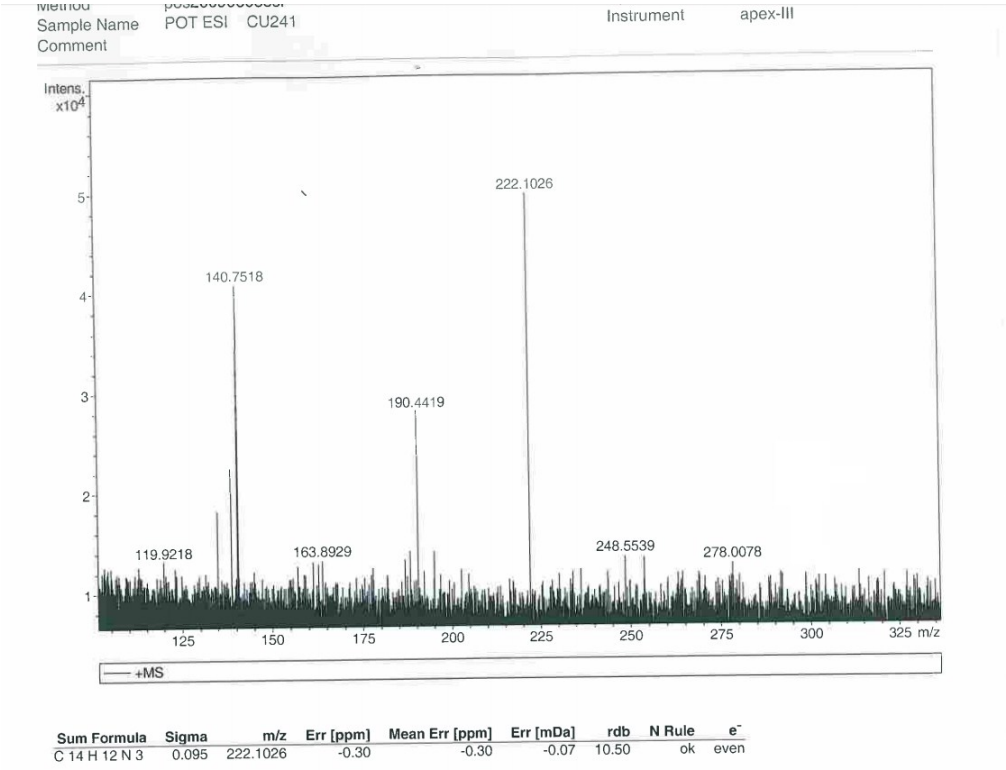

Figure S71. HRMS spectrum of triazole **18ca**.

(1-phenyl-1H-1,2,3-triazol-4-yl)methanol (18cc)[7]

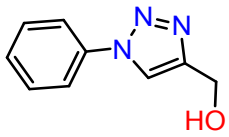

Light yellow oil; ^{1}H NMR (600 MHz, $CDCl_3$) δ 7.98 (s, 1H), 7.73 (d, J = 7.6 Hz, 2H), 7.53 (t, J = 7.8 Hz, 2H), 7.45 (t, J = 7.5 Hz, 1H), 4.91 (s, 2H). ^{13}C NMR (151 MHz, $CDCl_3$) δ 148.21, 135.58, 129.78, 128.85, 120.61, 119.94, 56.71. HRMS for $C_9H_9N_3ONa$ [M + Na]: calc: 198.0638, found: 198.0631.

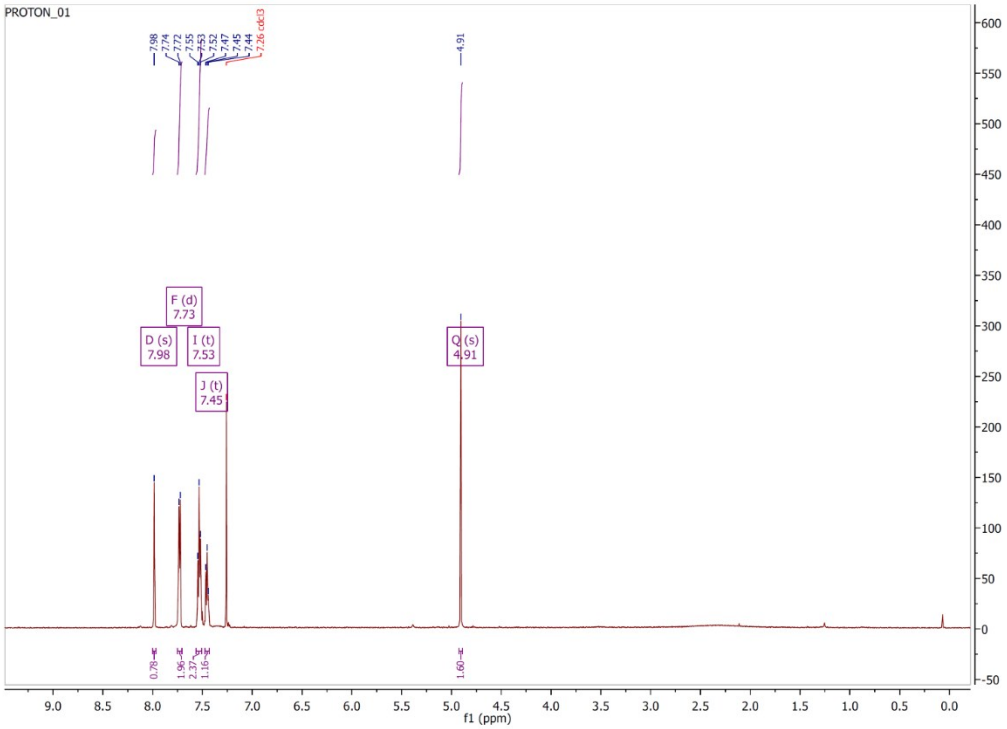

Figure S72. ^{1}H NMR spectrum of triazole **18cc**.

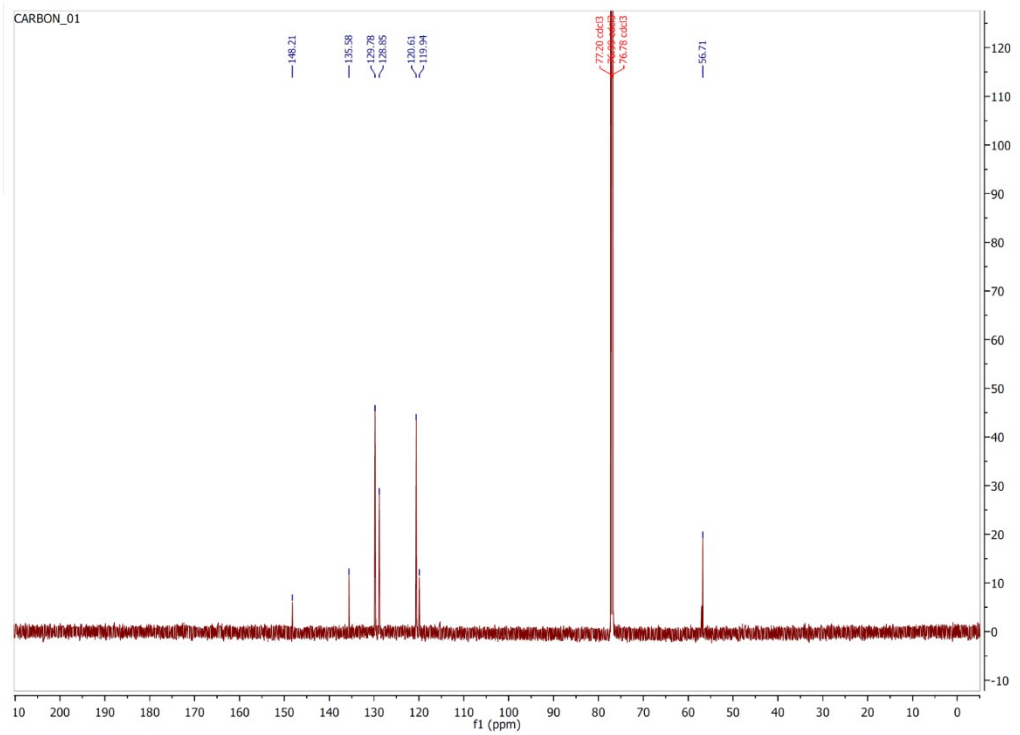

Figure S73. ^{13}C NMR spectrum of triazole **18cc**.

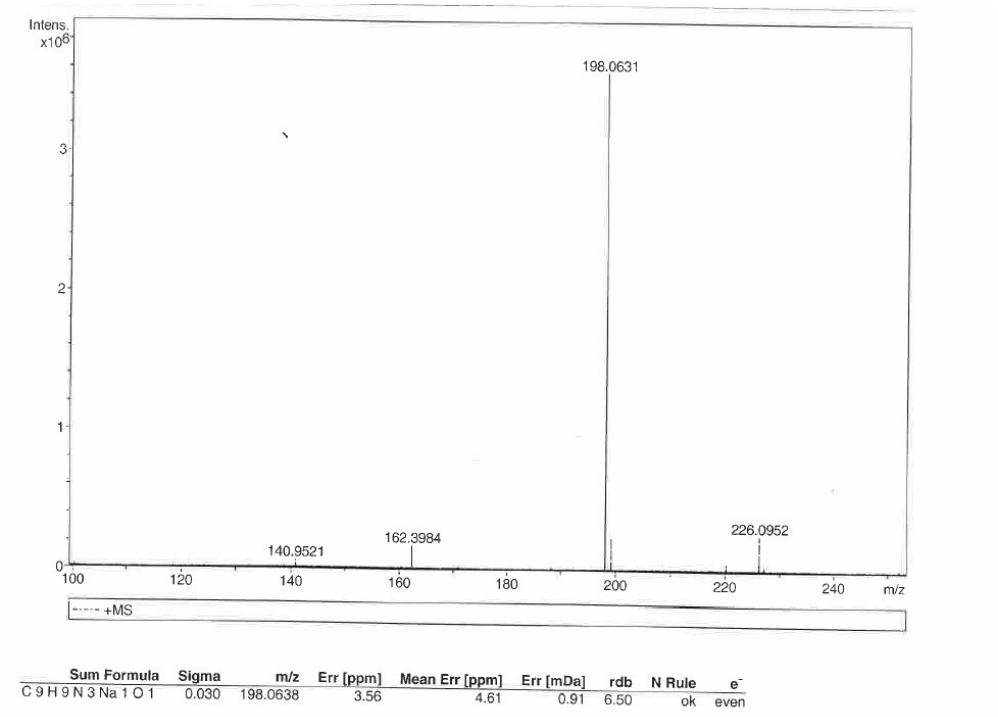

Figure S74. HRMS spectrum of triazole **18cc**.

2-(1-phenyl-1H-1,2,3-triazol-4-yl)ethanol (18cd)[8]

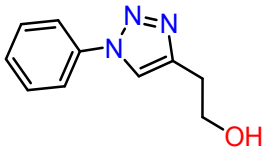

Light yellow oil; ^{1}H NMR (600 MHz, $CDCl_3$) δ 7.85 (s, 1H), 7.73 (d, J = 7.9 Hz, 2H), 7.53 (t, J = 7.7 Hz, 2H), 7.44 (t, J = 7.2 Hz, 1H), 4.03 (t, J = 5.9 Hz, 2H), 3.21 (t, J = 6.3 Hz, 1H), 3.06 (t, J = 5.8 Hz, 2H). ^{13}C NMR (151 MHz, $CDCl_3$) δ 146.20, 135.61, 129.72, 128.67, 120.49, 119.84, 77.20, 76.99, 76.78, 61.62, 28.69. HRMS for $C_{10}H_{11}N_3ONa$ [M + Na]: calc: 212.0794, found: 212.0786.

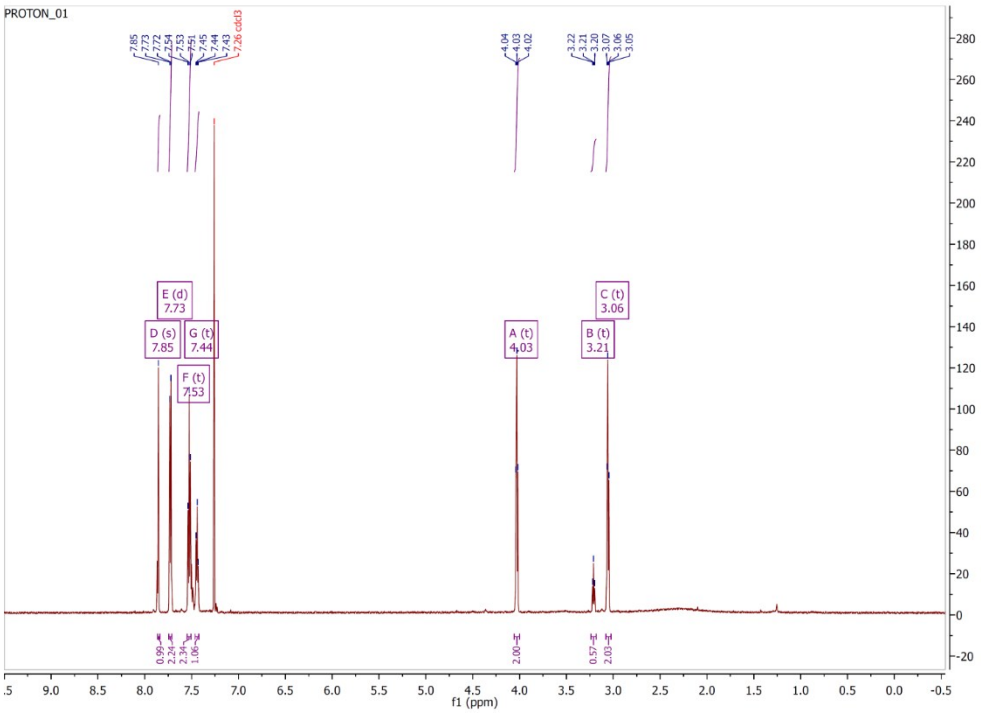

Figure S75. ^{1}H NMR spectrum of triazole **18cd**.

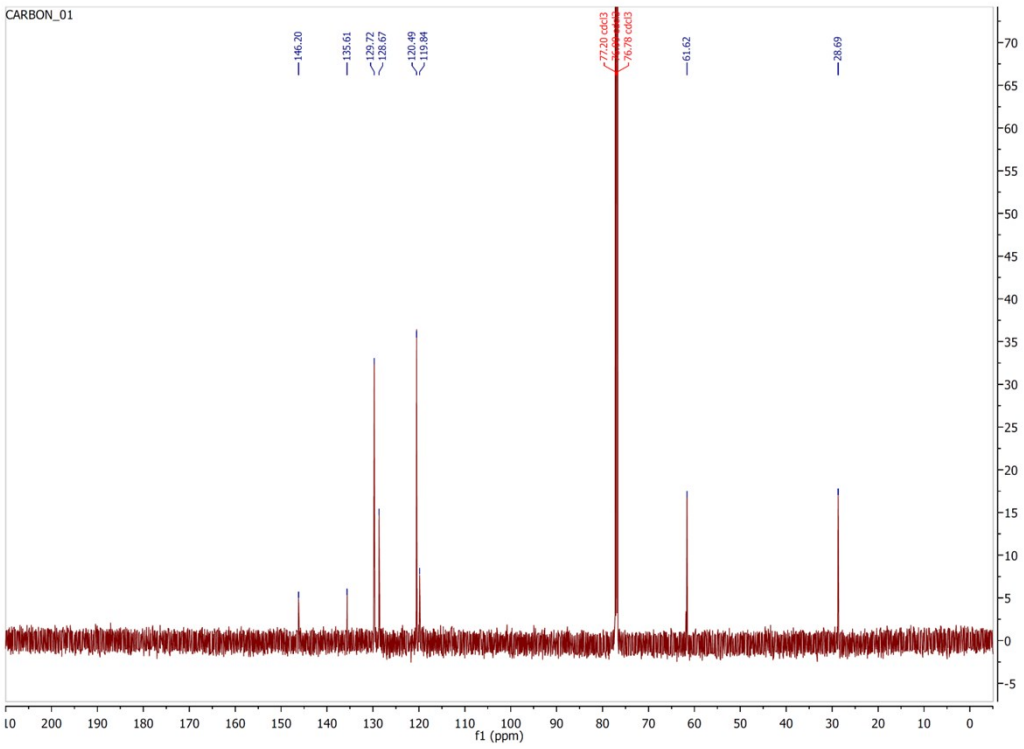

Figure S76. ^{13}C NMR spectrum of triazole **18cd**.

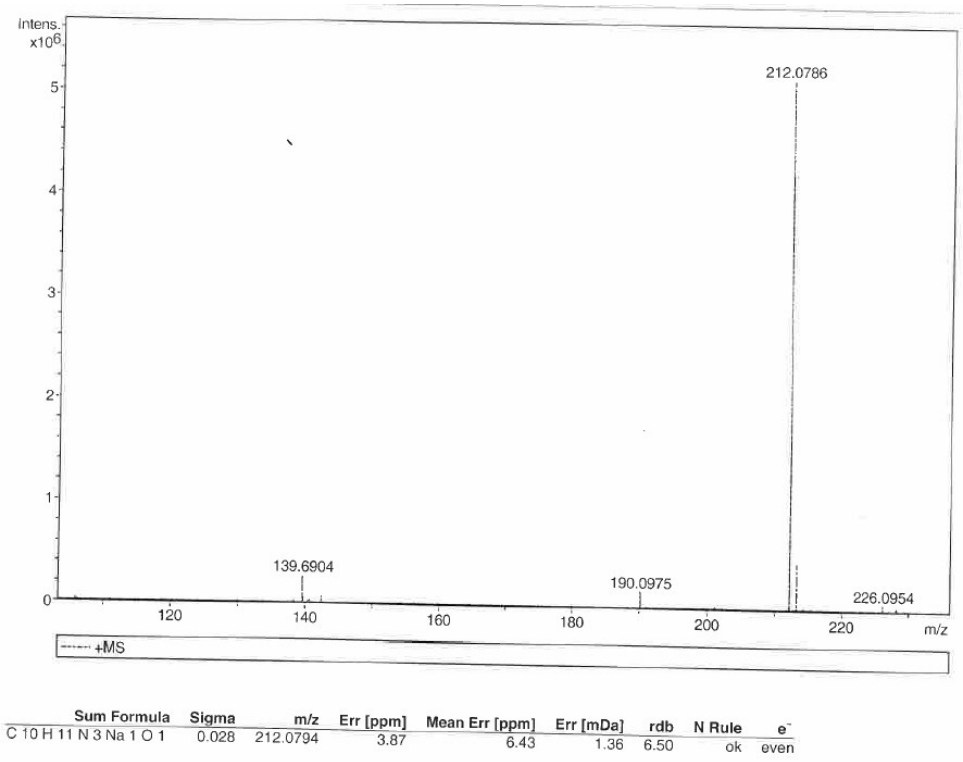

Sum Formula	Sigma	m/z	Err [ppm]	Mean Err [ppm]	Err [mDa]	rdb	N Rule	e⁻
C 10 H 11 N 3 Na 1 O 1	0.028	212.0794	3.87	6.43	1.36	6.50	ok	even

Figure S77. HRMS spectrum of triazole **18cd**.

References

1 Y. C. Wang, Y. Y. Xie, H. E. Qu, H. S. Wang, Y. M. Pan and F. P. Huang, *J. Org. Chem.*, 2014, **79**, 4463–4469.

2 A. Taher, D. Nandi, R. U. Islam, M. Choudhary and K. Mallick, *RSC Adv.*, 2015, **5**, 47275–47283.

3 Y. Wang, J. Liu and C. Xia, *Adv. Synth. Catal.*, 2011, **353**, 1534–1542.

4 J. Shah, S. S. Khan, H. Blumenthal and J. Liebscher, *Synthesis (Stuttg).*, 2009, **2009**, 3975–3982.

5 K. Chanda, S. Rej and M. H. Huang, *Chem. - A Eur. J.*, 2013, **19**, 16036–16043.

6 S. Kaur, V. Bhalla and M. Kumar, *Chem. Commun.*, 2015, **51**, 526–529.

7 H. Hagiwara and S. Okada, *Chem. Commun.*, 2016, **52**, 815–818.

8 Y. Jiang, X. He, W. Zhang, X. Li, N. Guo, Y. Zhao, G. Xu and W. Li, *RSC Adv.*, 2015, **5**, 73340–73345.